[redacted]
April 1977

CRITICAL HEAT FLUX AND TRANSITION BOILING CHARACTERISTICS FOR A SODIUM-HEATED STEAM GENERATOR TUBE FOR LMFBR APPLICATION

S. Wolf and D. H. Holmes

Approved: P. M. Magee
P. M. Magee, Manager
Steam Generator Development

Approved: F. E. Tippets
F. E. Tippets, Manager
Component Development

Prepared for PLBR Project, FBRD, GE
Under Development Authorization No. PH288

FAST BREEDER REACTOR DEPARTMENT ● GENERAL ELECTRIC COMPANY
SUNNYVALE, CALIFORNIA 94086

GENERAL ELECTRIC

65p/45 -- SGD
rap -- 4/77

DISCLAIMER

TABLE OF CONTENTS

ABSTRACT vii

ACKNOWLEDGMENTS viii

1. INTRODUCTION 1

2. TEST SECTION AND TEST FACILITY 2

3. EXPERIMENTAL PROCEDURES 6

4. DATA REDUCTION 7
   4.1 Thermocouple Calibration 7
   4.2 Shell Temperature 7
   4.3 Bulk Sodium Temperature, Heat Flux and CHF Location 7

5. RESULTS 14
   5.1 CHF Correlation 14
   5.2 Transition Boiling Characteristics 28

NOMENCLATURE 34

REFERENCES 35

APPENDIX A: SUMMARY OF CHF DATA A-1

APPENDIX B: TEMPERATURE AND HEAT FLUX DISTRIBUTIONS WITH CHF. B-1

DISTRIBUTION C-1

LIST OF ILLUSTRATIONS

Figure	Title	Page
1	Schematic Representation of Test Section	3
2	Schematic Representation of Test Facility	4
3	Test Section Instrumentation	5
4a	Typical Results from Data Reduction Program	8
4b	Input Data--DNB Effects Test Program THAN	9
4c	Basic Data--DNB Effects Test Program THAN	10
4d	Correlating Data #1--DNB Effects Test Program THAN	11
4e	Correlating Data #2--DNB Effects Test Program THAN	12
5	Critical Heat Flux Versus Critical Steam Quality for High-Mass Flux at P_C = 7.2 MPa (1040 psia)	16
6	Critical Steam Quality Versus Mass Flux at P_C = 7.2 MPa	17
7	Comparison of Experimental Critical Steam Quality for High-Mass Flux at P_C = 7.2 MPa with Predictions	
	a. CISE Correlation	18
	b. Doroschuk Correlation	18
	c. Westinghouse-Hwang Correlation	19
	d. GE-1976 Correlation	19
8	Comparison of GE Critical Quality Data with Correlation, Equation (4)	21
9	Comparison of ANL Critical Steam Quality Data with Correlation, Equation (4)	22
10	Comparison of GE and ANL Data for G and P_C Conditions Simulating Proposed PLBR Steam Generator Conditions	23
11	Critical Heat Flux versus Critical Steam Quality for G = 260 kg/s·m^2 (0.20×10^6 lbm/h·ft^2) and P_C = 7.2 MPa	24
12	Critical Heat Flux versus Critical Steam Quality for G = 130 kg/s·m^2 (0.10×10^6 lbm/h·ft^2) and P_C = 7.2 MPa	25
13	Effect of Diameter on Critical Steam Quality	27
14	Tube Wall Outer Surface Temperature Behavior Near CHF for High-Mass Flux	29
15	Tube Wall Surface Temperature Behavior Near CHF for Low-Mass Flux	30
B-1	Heat Flux and Temperature Distribution, Test 20.3, G = 1440 kg/s·m^2	B-2
B-2	Heat Flux and Temperature Distribution, Test 21.2, G = 1485 kg/s·m^2	B-3
B-3	Heat Flux and Temperature Distribution, Test 22.3, G = 1334 kg/s·m^2	B-4
B-4	Heat Flux and Temperature Distribution, Test 23.3, G = 1327 kg/s·m^2	B-5
B-5	Heat Flux and Temperature Distribution, Test 24.5, G = 1098 kg/s·m^2	B-6

LIST OF ILLUSTRATIONS (Continued)

Figure	Title	Page
B-6	Heat Flux and Temperature Distribution, Test 25.5, G = 1089 kg/s•m^2	B-7
B-7	Heat Flux and Temperature Distribution, Test 26.7, G = 810 kg/s•m^2	B-8
B-8	Heat Flux and Temperature Distribution, Test 27.5, G = 819 kg/s•m^2	B-9
B-9	Heat Flux and Temperature Distribution, Test 28.6, G = 590 kg/s•m^2	B-10
B-10	Heat Flux and Temperature Distribution, Test 29.6, G = 552 kg/s•m^2	B-11
B-11	Heat Flux and Temperature Distribution, Test 30.6, G = 262 kg/s•m^2	B-12
B-12	Heat Flux and Temperature Distribution, Test 31.6, G = 264 kg/s•m^2	B-13
B-13	Heat Flux and Temperature Distribution, Test 34.4, G = 263 kg/s•m^2	B-14
B-14	Heat Flux and Temperature Distribution, Test 32.7, G = 133 kg/s•m^2	B-15
B-15	Heat Flux and Temperature Distribution, Test 35.3, G = 117 kg/s•m^2	B-16
B-16	Heat Flux and Temperature Distribution, Test 36.5, G = 132 kg/s•m^2	B-17

LIST OF TABLES

Table	Title	Page
A-1	CHF Results for High Mass Flux at 7.2 MPa	A-2
A-2	CHF Results for Low Mass Flux at 7.2 MPa	A-3

ABSTRACT

An experimental program was conducted to characterize critical heat flux (CHF) in a sodium-heated steam generator tube model at a proposed PLBR steam generator design pressure of 7.2 MPa. Water was circulated vertically upward in the tube and the heating sodium was flowing counter-current downward. The experimental ranges were: mass flux, 110 to 1490 kg/s·m^2 (0.08 to 1.10 10^6 lbm/h·ft^2); critical heat flux, 0.16 to 1.86 MW/m^2 (0.05 to 0.59 10^6 Btu/h·ft^2); and critical quality, 0.48 to 1.0. The CHF phenomenon for the experimental conditions is determined to be dryout as opposed to departure from nucleate boiling (DNB). The data are divided into high- and low-mass flux regions. The high-mass flux data and dryout data obtained previously from the same sodium-heated test facility are correlated. The resulting correlation extends over a pressure range of 7.0 to 13.0 MPa (1015 to 1890 psia) and mass flux range of 540 to 3250 kg/s·m^2 (0.40 to 2.40 10^6 lbm/h·ft^2). The length of the transition boiling region is also determined for selective high- and low-mass flux conditions.

1. INTRODUCTION

The steam generator for the PLBR plant proposed by GE is designed to operate at full power at about 7.2 MPa (1040 psia) outlet pressure, 1500 kg/s m^2 (1.1 x 10^6 lbm/h·ft^2) mass flux and 17% outlet quality. The steam generator is designed to avoid critical heat flux (CHF) based on the use of existing Westinghouse-Hwang[1] critical quality correlation. This correlation was selected because at the start of the PLBR design phase it represented the largest experimental data base obtained from a sodium-heated test section at conditions near the proposed PLBR steam generator design. However, some extrapolation to conditions not covered in the Westinghouse test is required. Consequently, tests have been conducted at ANL and GE to produce data at conditions applicable to the proposed PLBR steam generator design. Preliminary test results[2] were first obtained in November 1976 in the GE-DNB Loop during shutdown procedures of the GE-DNB Effects test.[3] A test matrix for CHF tests covering both nominal and reduced water mass fluxes was planned for a second test section installed in the GE-DNB Loop during January 1977. These latter tests were completed in February 1977.

The ANL Steam Generator Test Facility (SGTF) has been used during 1976 to generate data to support the CRBRP steam generator design. The SGTF has a 13.1 m (43 ft) test section compared to a 4.88 m (16 ft) test section in the GE-DNB Loop and, consequently, lower critical heat flux conditions can be achieved in the SGTF loop than in the DNB loop for prescribed high-mass flux conditions. CHF tests covering proposed PLBR thermal-hydraulic conditions are planned at ANL in early 1977. These tests are planned to complement the GE data and provide a large data base to support the proposed PLBR steam generator design.

This report summarizes the GE-CHF test results. The CHF data are divided into high- and low-mass flux regions and compared with several CHF correlations available in the technical literature. A new simple correlation is formulated to represent the current high-mass flux data and data previously obtained[3] from the same sodium-heated test facility during the GE-DNB Effects program.

Characteristics of the transition boiling region for selective high- and low-mass flux conditions are described, and the length of the region is determined, based on thermocouples mounted on the outside surface of the tube wall for selected high- and low-mass flux conditions.

2. TEST SECTION AND TEST FACILITY

The test section consists of a hockey-stick shaped central tube of 10.1 mm (0.398 in.) inside diameter by 15.8 mm (0.624 in.) outside diameter enclosed by an outer shell as schematically represented in Figure 1. The tube has a straight 4.88 m (16.0 ft) active heating length defined as the section between the center lines of the sodium outlet and the sodium inlet nozzles. Over the active length, the tube is enclosed by a 35.0 mm (1.38 in.) inside diameter shell. Both the central tube and the surrounding shell are fabricated from 2-1/4Cr-1Mo. The tube is centered by 4 small 3-pin spacers located at 0.78, 1.77, 2.52, and 3.28 m and a prototypical LMFBR plant spacer at 4.27 m from the active water inlet section. Temperature wells containing Resistant Thermal Devices (RTDs) are located in the sodium and water inlets and outlets. Pressure taps are located at the water inlet and outlet. The test section is insulated to reduce heat losses and measurement errors.

The test article was installed in the experimental facility shown schematically in Figure 2. Water is circulated vertically upward in the test section and is heated by downward flowing sodium. The sodium is electrically heated and is circulated by an electromagnetic pump. The sodium flow is measured with an electromagnetic flow meter and the water flow with a venturi meter. Additional details of the test article and test facility are contained in References 3 to 5.

The test article instrumentation[6] consists of 92 thermocouples mounted on the outer shell and 6 thermocouples on the outer surface of the inner tube, as schematically represented in Figure 3. The shell thermocouples are arranged with variable axial spacing of 30.5 cm (12 in.) near the water inlet end and 5.1 cm (2 in.) over the region from z = 3.05 to 4.42 m (10.0 to 14.5 ft) measured from the active water inlet section. Two thermocouples are mounted at each axial location and spaced 180^{o} circumferentially.

Two sets of 3 thermocouples are mounted on the outside surface of the tube wall. The sets are centered at 4.72 and 4.88 m (15.5 and 16.0 ft) from the active water inlet section. The individual thermocouples in each set are spaced 15.9 mm (0.625 in.) axially and 120^{o} circumferentially as illustrated in Figure 1. Each thermocouple is held in place with a mounting block, 3.2 mm deep by 6.4 mm wide by 11.4 mm long, tightly strapped to the outer tube surface. The tube thermocouples are fabricated from 2.3 mm (0.09 in.) diameter wire flattened to about 1.1 mm (0.043 in.) in a cavity within each block.

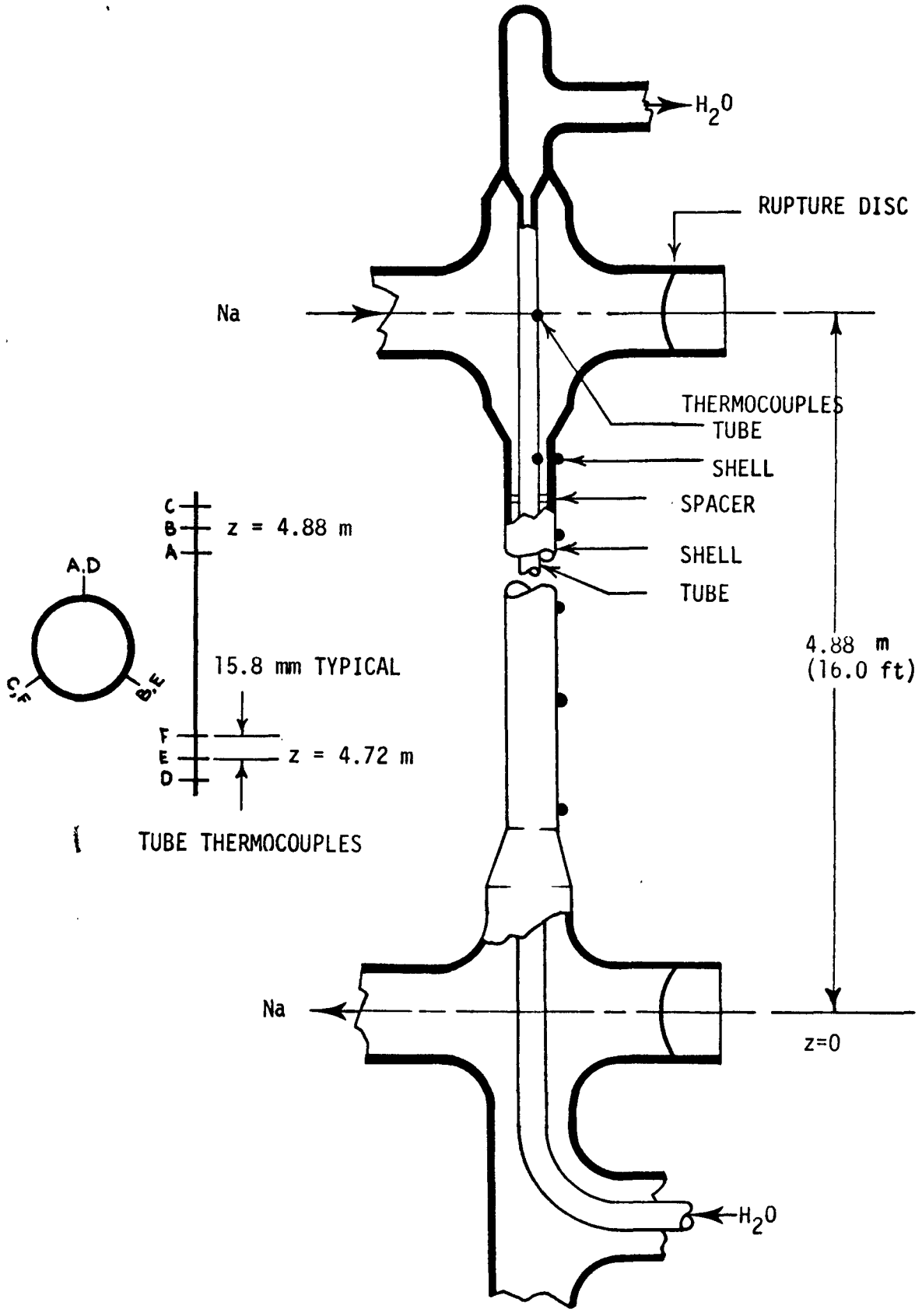

Figure 1. Schematic Representation of Test Section

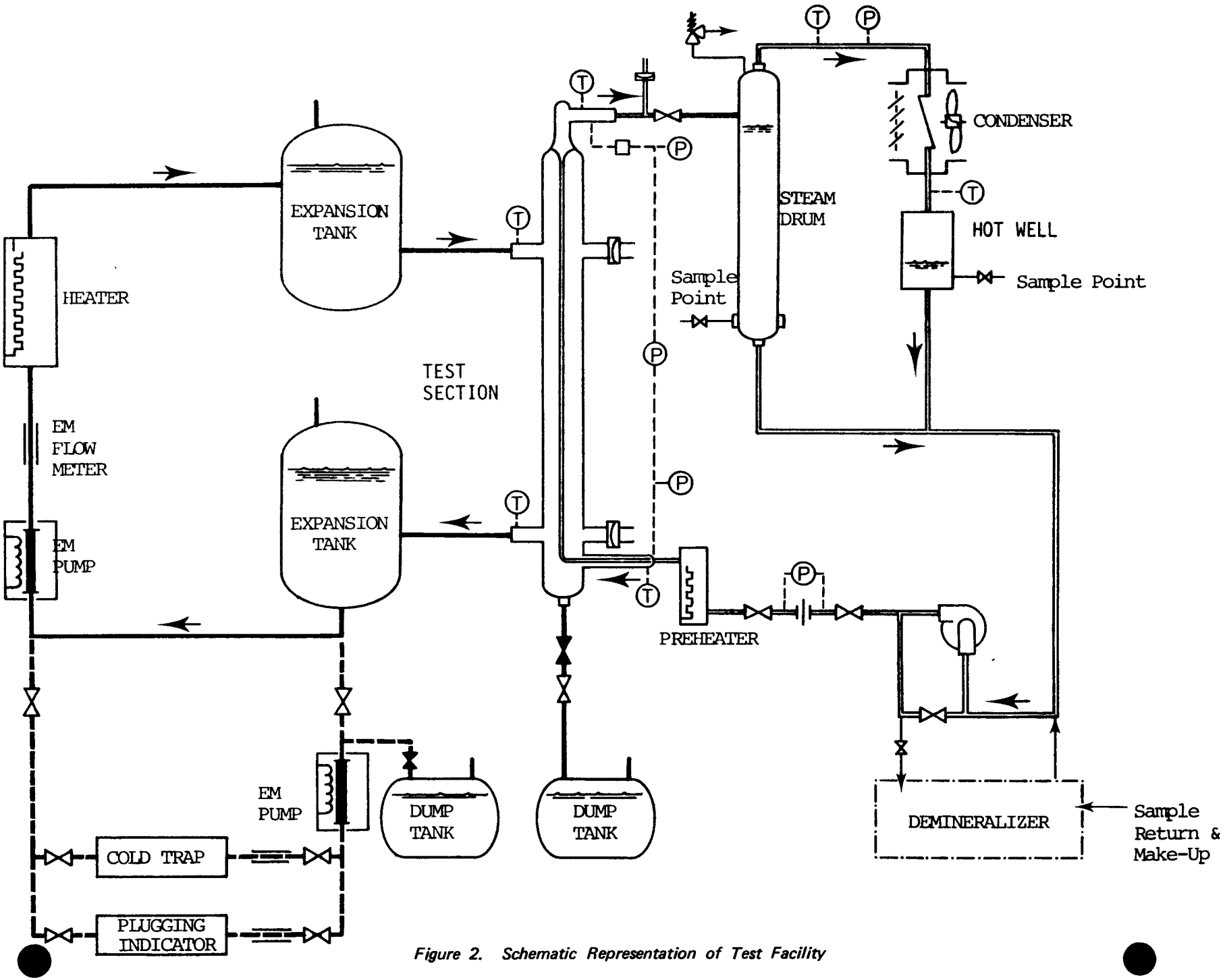

Figure 2. Schematic Representation of Test Facility

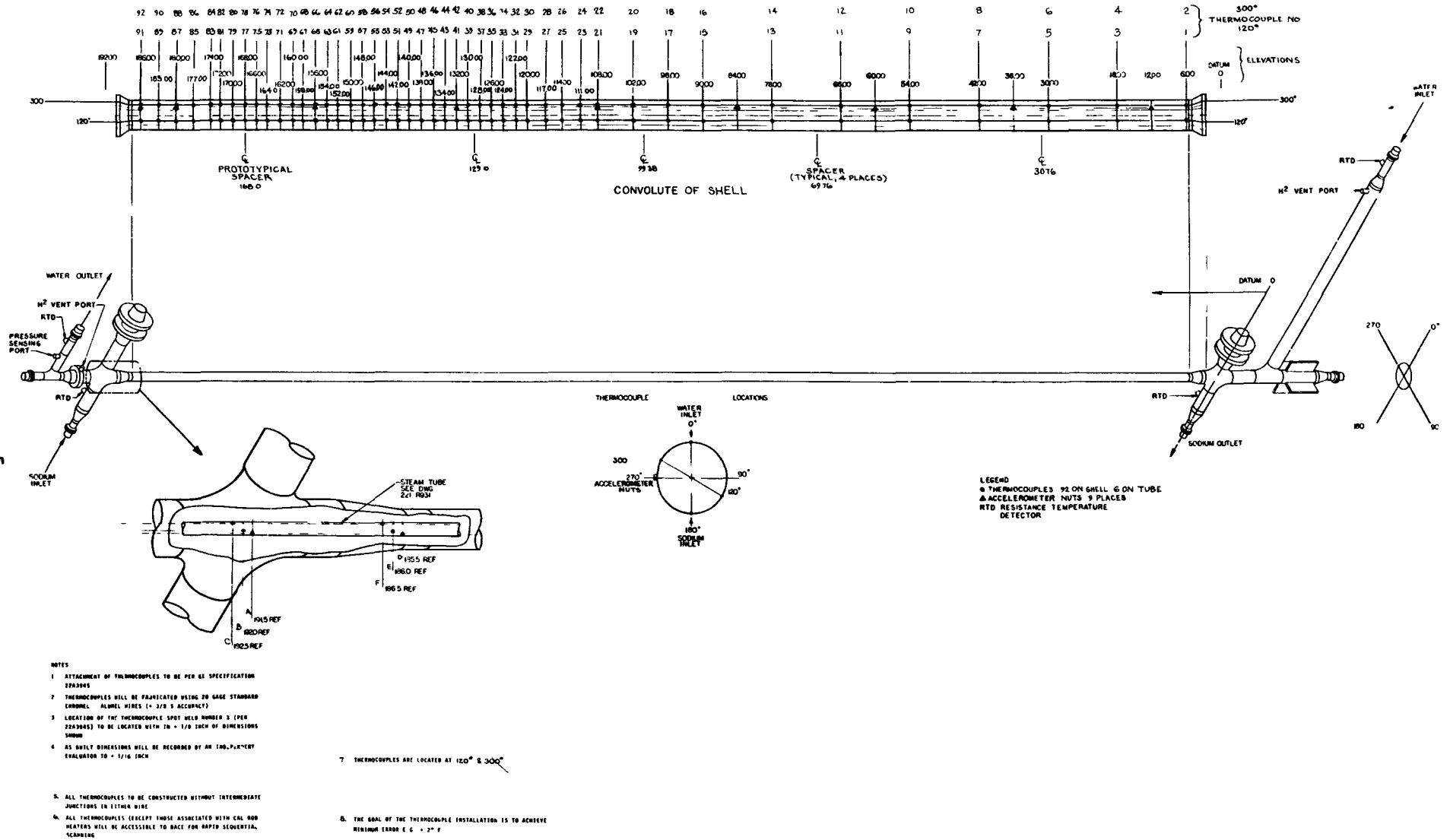

NOTES

1. ATTACHMENT OF THERMOCOUPLES TO BE PER GE SPECIFICATION 22A3945
2. THERMOCOUPLES WILL BE FABRICATED USING 20 GAGE STANDARD CHROMEL ALUMEL WIRES (± 3/8 % ACCURACY)
3. LOCATION OF THE THERMOCOUPLE SPOT WELD NUMBER 3 (PER 22A3945) TO BE LOCATED WITH IN ± 1/8 INCH OF DIMENSIONS SHOWN
4. AS BUILT DIMENSIONS WILL BE RECORDED BY AN IND. PARTY EVALUATOR TO ± 1/16 INCH
5. ALL THERMOCOUPLES TO BE CONSTRUCTED WITHOUT INTERMEDIATE JUNCTIONS IN EITHER WIRE
6. ALL THERMOCOUPLES (EXCEPT THOSE ASSOCIATED WITH CAL ROD HEATERS) WILL BE ACCESSIBLE TO BACE FOR RAPID SEQUENTIAL SCANNING
7. THERMOCOUPLES ARE LOCATED AT 120° & 300°
8. THE GOAL OF THE THERMOCOUPLE INSTALLATION IS TO ACHIEVE MINIMUM ERROR ± 2° F

Figure 3. Test Section Instrumentation

3. EXPERIMENTAL PROCEDURES

Pressure transducers used in the DNB Test Loop were calibrated with on-line digital readout equipment against calibrated pressure standards. The RTDs were calibrated out of the test facility in an independent laboratory to an uncertainty of $\pm 0.1^{\circ}C$. The shell and tube wall thermocouples were calibrated by using the sodium inlet and outlet RTDs as standard references during isothermal sodium runs. The isothermal runs were conducted at 288°, 385°, and $482^{\circ}C$ (550°, 725°, and $900^{\circ}F$) and sodium flow rates corresponding to the minimum and maximum flow rates for the test matrix. The results of the isothermal calibrations were used to determine calibration constants for the shell and tube wall thermocouples and heat losses for the test article.

Tests were conducted at seven different water flow rates from 140 to 1490 $kg/s \cdot m^2$ (0.1 to 1.1 10^6 $lbm/h \cdot ft^2$) with 7.24 MPa (1050 psia) nominal test section inlet pressure and 16 J/g (7 Btu/lb) nominal inlet subcooling. At each water flow rate a test series was conducted with the sodium flow rate specified and the sodium inlet temperature was increased until temperature oscillations were observed with the tube-mounted thermocouples at z = 4.88 m (16.0 ft) indicating CHF at this location. The system was then stabilized, and with the tube thermocouples at z = 4.88 m (16.0 ft) still oscillating, the data were collected on the data acquisition system. The next test condition in a test series was obtained by further increasing the sodium inlet temperature until the temperature oscillations were observed with the tube thermocouples at z = 4.72 m (15.5 ft). Additional runs for each test series were obtained by further increasing the sodium inlet temperature to move CHF down the tube.

A total of up to 10 data scans (8 normal) were repeated for each test condition. For each data scan a total of 111 experimental measurements were collected with an HP-2114a data acquisition system in 8 seconds. The data were punched out on a paper tape for reduction with a timeshare terminal. For each test, the system was allowed to stabilize to a steady-state condition before the scans were initialized.

4. DATA REDUCTION

A computer program, called THAN-PLBR, modified from the Thermal-Hydraulic Analysis computer program, THAN, was used to process the test data to provide heat flux, heat transfer coefficients, and steam or water properties for various positions along the test section and at the CHF point.

Prior to data treatment with THAN-PLBR, the shell and tube thermocouples were calibrated by using a separate computer program. This calibration procedure and some of the specific tasks performed by the computer program THAN-PLBR are discussed in the following subsections. A more complete description of THAN is contained in Reference 3. A sample output from THAN-PLBR is presented in Figure 4.

4.1 THERMOCOUPLE CALIBRATION

The shell and tube wall thermocouples were calibrated by using the sodium inlet and outlet RTDs as standard references. During this calibration, the test section heat losses were experimentally determined. To accomplish these tasks, data were obtained at three different temperatures and nearly isothermal, steady-state sodium flow without water or steam in the tube. These data were used in a computer program that calculates the calibration constants and heat losses and stores them in the form of the constants of quadratic equations. This calibration procedure was performed both prior to and immediately following the CHF test series. There was no significant variation between the results of the two calibrations. Additional details on the calibration procedure are described in Reference 3.

4.2 SHELL TEMPERATURE

The corrected shell temperatures are averaged at each station. The averaged temperatures are fitted with a smooth fourth-order spline curve. The spline curve can be based on a prescribed number of data points to limit the curve smoothing, thereby forcing the spline function and the temperature points to agree within a specified tolerance. Sets of 6 points were selected for the spline curve to fit the shell temperature.

4.3 BULK SODIUM TEMPERATURE, HEAT FLUX AND CHF LOCATION

The sodium bulk temperature, T_N, is determined from the average shell temperature, T_S, at each station from iteration with 2 equations. One equation is:

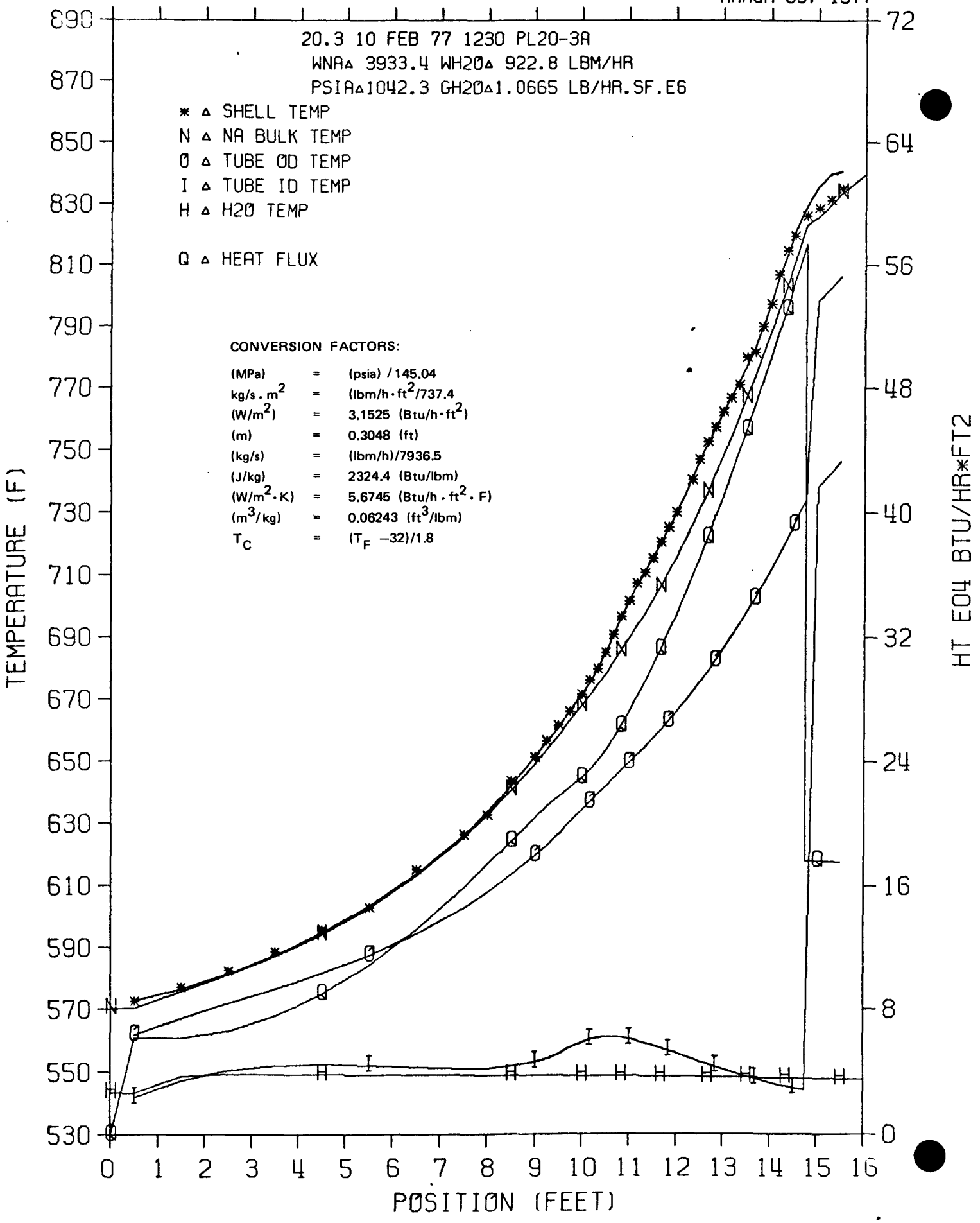

Figure 4a. Typical Results from Data Reduction Program

INPUT DATA--DNB EFFECTS TEST PROG "THAN"
20.3 10 FEB 77 1230 PL20-3A

SENSOR LOCAT* STATION	(FT)*	TEMPERATURE (F) TC300	TC120	AVG	SMOOTH CURVE	SMOOTH CURVE AVG	MINUS TC300	TC120
1	0.500	571.8	572.3	572.0	572.6	0.57	0.85	0.29
2	1.500	575.5	577.6	576.6	576.3	-0.27	0.76	-1.30
3	2.500	580.4	583.3	581.9	581.3	-0.60	0.88	-2.09
4	3.500	585.9	590.6	588.2	587.4	-0.86	1.49	-3.21
5	4.500	592.2	598.4	595.3	594.8	-0.51	2.60	-3.64
6	5.500	599.3	605.6	602.4	603.5	1.05	4.22	-2.13
7	6.500	611.3	618.0	614.7	613.6	-1.10	2.24	-4.46
8	7.500	622.9	628.9	625.9	626.1	0.17	3.15	-2.83
9	8.000	629.3	635.3	632.3	633.6	1.32	4.30	-1.68
10	8.500	639.9	646.3	643.1	642.1	-1.05	2.14	-4.25
11	9.000	647.6	654.4	651.0	651.3	0.38	3.77	-3.04
12	9.250	653.4	0.	656.2	656.0	-0.12	2.69	656.04
13	9.500	658.8	663.6	661.2	660.8	-0.44	1.93	-2.82
14	9.750	663.2	667.8	665.5	665.8	0.32	2.66	-2.02
15	10.000	0.	672.5	671.1	671.3	0.19	671.31	-1.14
16	10.167	674.2	677.5	675.8	675.3	-0.55	1.10	-2.19
17	10.333	678.5	680.2	679.4	679.7	0.37	1.22	-0.49
18	10.500	685.0	684.2	684.6	684.8	0.20	-0.21	0.61
19	10.667	692.0	688.8	690.4	690.3	-0.10	-1.72	1.52
20	10.833	696.5	696.0	696.2	695.9	-0.29	-0.54	-0.03
21	11.000	701.5	700.9	701.2	701.4	0.15	-0.14	0.44
22	11.167	709.0	704.8	706.9	706.3	-0.63	-2.76	1.49
23	11.333	710.1	710.5	710.3	710.8	0.53	0.72	0.34
24	11.500	715.3	714.6	715.0	715.3	0.35	0.01	0.69
25	11.667	720.5	719.7	720.1	719.9	-0.18	-0.61	0.26
26	11.833	724.7	725.3	725.0	724.7	-0.31	-0.04	-0.58
27	12.000	729.1	730.5	729.8	729.6	-0.15	0.53	-0.84
28	12.333	737.4	742.4	739.9	740.5	0.64	3.11	-1.85
29	12.500	744.9	748.2	746.5	746.3	-0.27	1.36	-1.90
30	12.667	750.8	753.7	752.3	751.8	-0.44	1.03	-1.92
31	12.833	0.	759.2	757.0	757.0	-0.03	756.98	-2.26
32	13.000	758.8	764.9	761.8	761.7	-0.12	2.95	-3.19
33	13.167	763.9	0.	766.3	766.6	0.32	2.71	766.60
34	13.333	768.6	772.5	770.5	771.7	1.20	3.14	-0.75
35	13.500	768.9	779.5	779.5	777.1	-2.39	8.17	-2.39
36	13.667	776.4	0.	781.2	782.6	1.44	6.17	782.61
37	13.833	0.	792.4	789.5	789.6	0.01	789.56	-2.86
38	14.000	796.9	829.3	796.9	797.5	0.58	0.58	-31.84
39	14.167	803.8	809.2	806.5	805.8	-0.76	1.94	-3.46
40	14.333	812.8	815.9	814.3	813.3	-1.01	0.56	-2.59
41	14.500	819.3	822.1	819.2	819.6	0.38	0.28	-2.53
42	14.750	824.2	827.2	825.7	826.6	0.82	2.33	-0.69
43	15.000	826.4	830.0	828.2	830.9	2.62	4.42	0.82
44	15.250	829.4	832.5	830.9	832.9	1.97	3.50	0.43
45	15.500	832.4	836.5	834.5	833.0	-1.48	0.58	-3.55

	SODIUM		H2O	
FLOW RATE =	3933.4 / 5.7		922.8 / 872.0	(LBM/HR) / MV
TEMP IN =	839.9 / 839.9		543.4 / 543.4	(F)
TEMP OUT =	570.2 / 570.2		548.4 / 548.4	(F)
PRESS IN =			1042.3 / 695.3	(PSIA)
PRESS OUT =			1035.7 / 693.1	(PSIA)
PRESS DROP=			17.29 / 389.94	(PSI)
TEMPERATURES				
FLOW METER=	570.2 / 836.5		536.8 / 8.7	(F)
CONDENSER =			520.6 / 8.4	(F)
PUMP INLET=			538.5 / 8.8	(F)

TUBE T.C. #1 = 856.1 #2 = 834.9 #3 = 788.6 (F)
#4 = 840.4 #5 = 830.2 #6 = 832.2 (F)

TUBE ID = 0.3983 TUBE OD = 0.6240 SHELL ID = 1.3800 INCHES

Figure 4b.

BASIC DATA--DNB EFFECTS TEST PROG "THAN"
20.3 10 FEB 77 1230 PL20-3A

LOCAT (FT)	BOIL LENGTH	*TEMPERATURES *SHELL	NA	OD	ID	H2O	*H2O PROPERTIES *QUALITY	VOID	PSIA	ENTHALP BTU/LBM	*HEAT FLUX *BTU/HR.FT2
-0.75	-2.39	0	570.2	0.	0.	543.4	0.	0.	1042.3	541.2	0.
0.50	-1.14	572.6	570.2	561.6	541.7	543.1	0.	0.	1041.1	540.8	61260.
1.50	-0.14	576.3	575.6	566.9	547.1	548.5	0.	0.	1039.9	547.6	61052.
1.641			********NUCLEATE BOILING********								
1.64	0.	577.0	576.3	567.6	547.6	549.2	0.0001	0.001	1039.8	548.6	61720.
2.50	0.86	581.3	581.1	571.8	550.4	549.2	0.0096	0.140	1039.4	554.8	65783.
3.50	1.86	587.4	587.2	576.5	551.9	549.2	0.0221	0.268	1038.9	562.7	75401.
4.50	2.86	594.8	594.3	581.5	552.3	549.1	0.0366	0.373	1038.4	572.0	89706.
5.50	3.86	603.5	602.8	587.3	552.0	549.0	0.0541	0.460	1037.9	583.2	108456.
6.50	4.86	613.6	613.1	594.3	551.4	549.0	0.0752	0.535	1037.4	596.7	131498.
7.50	5.86	626.1	625.6	602.8	551.0	548.9	0.1008	0.599	1036.8	613.0	158773.
8.00	6.36	633.6	632.8	607.7	551.1	548.8	0.1155	0.627	1036.4	622.4	173546.
8.50	6.86	642.1	640.6	613.3	551.8	548.8	0.1314	0.653	1036.1	632.7	188358.
9.00	7.36	651.3	649.0	619.5	553.0	548.8	0.1487	0.677	1035.7	643.7	203453.
9.25	7.61	656.0	653.5	622.9	553.9	548.7	0.1578	0.688	1035.5	649.6	210690.
9.50	7.86	660.8	658.1	626.5	555.5	548.7	0.1673	0.699	1035.3	655.6	217011.
9.75	8.11	665.8	662.9	630.4	557.3	548.7	0.1769	0.709	1035.1	661.8	222882.
10.00	8.36	671.3	667.8	634.3	559.1	548.7	0.1869	0.719	1034.9	668.2	229369.
10.17	8.53	675.3	671.2	636.9	559.9	548.6	0.1937	0.725	1034.7	672.6	234392.
10.33	8.69	679.7	674.6	639.4	560.5	548.6	0.2007	0.731	1034.6	677.0	240193.
10.50	8.86	684.8	678.1	641.9	560.8	548.6	0.2078	0.737	1034.4	681.6	246874.
10.67	9.03	690.3	681.7	644.4	560.9	548.6	0.2152	0.743	1034.2	686.3	254205.
10.83	9.19	695.9	685.5	646.9	560.7	548.6	0.2228	0.749	1034.1	691.2	262213.
11.00	9.36	701.4	689.3	649.4	560.3	548.5	0.2306	0.754	1033.9	696.2	271079.
11.17	9.53	706.3	693.3	651.9	559.6	548.5	0.2387	0.760	1033.7	701.4	280682.
11.33	9.69	710.8	697.5	654.5	558.9	548.5	0.2470	0.766	1033.5	706.8	290757.
11.50	9.86	715.3	701.7	657.2	558.1	548.5	0.2557	0.771	1033.3	712.4	301163.
11.67	10.03	719.9	706.2	659.9	557.3	548.4	0.2647	0.777	1033.1	718.1	311923.
11.83	10.19	724.7	710.8	662.6	556.5	548.4	0.2740	0.782	1032.9	724.1	323035.
12.00	10.36	729.6	715.6	665.8	555.7	548.4	0.2837	0.788	1032.7	730.3	334498.
12.33	10.69	740.5	725.6	672.1	554.0	548.4	0.3039	0.798	1032.3	743.3	358520.
12.50	10.86	746.3	730.9	675.4	553.2	548.3	0.3147	0.804	1032.0	750.2	370986.
12.67	11.03	751.8	736.4	678.9	552.4	548.3	0.3257	0.809	1031.8	757.3	383845.
12.83	11.19	757.0	742.1	682.4	551.6	548.3	0.3372	0.814	1031.5	764.6	397049.
13.00	11.36	761.7	748.0	686.1	550.8	548.2	0.3490	0.820	1031.3	772.3	410598.
13.17	11.53	766.6	754.1	690.0	550.0	548.2	0.3612	0.825	1031.0	780.1	424492.
13.33	11.69	771.7	760.4	694.0	549.2	548.2	0.3739	0.830	1030.7	788.2	438728.
13.50	11.86	777.1	766.9	698.1	548.5	548.1	0.3869	0.835	1030.4	796.6	453306.
13.67	12.03	782.6	773.6	702.4	547.8	548.1	0.4004	0.840	1030.1	805.3	468225.
13.83	12.19	789.6	780.6	706.8	547.1	548.1	0.4143	0.845	1029.8	814.3	483485.
14.00	12.36	797.5	787.8	711.4	546.5	548.0	0.4287	0.851	1029.4	823.5	499083.
14.17	12.53	805.7	795.2	716.2	545.9	548.0	0.4436	0.856	1029.1	833.1	515021.
14.33	12.69	813.5	802.8	721.1	545.3	547.9	0.4589	0.861	1028.7	842.9	531295.
14.50	12.86	820.4	810.7	726.2	544.8	547.9	0.4746	0.866	1028.3	853.1	547907.
14.75	13.11	829.2	823.1	734.2	544.2	547.9	0.4992	0.874	1027.7	868.9	573493.
14.75	13.11	829.2	822.4	733.6	543.5	547.8	0.4980	0.873	1027.7	868.0	573522.
14.750	13.109		********FILM BOILING********								
14.75	13.11	829.2	822.4	795.1	734.9	547.8	0.4980	0.873	1027.7	868.0	176169.
15.00	13.36	835.8	825.7	798.4	738.3	547.8	0.5043	0.875	1027.3	872.1	175839.
15.25	13.61	839.8	829.7	802.4	742.3	547.7	0.5121	0.878	1026.9	877.1	175488.
15.50	13.86	840.9	833.6	806.4	746.3	547.7	0.5197	0.880	1026.5	882.0	175123.
16.00	14.36	839.9	839.9	839.0	837.1	547.6	0.5323	0.884	1025.7	890.2	5512.

AVG NUCL BOIL HEAT FLUX = 215662. BTU/HR.SQFT.F
PWR SUBCOOLED = 2.009 NUCLEATE = 86.337 FILM = 5.981 TOTAL = 94.328 KW
DELTA T NUCL = 190.02 DELTA T FILM = 60.23 DELTA(DELTA T) = 129.79
QH2O=1036477. 1-PR=0.679656 HFG=645.16 QCR= 573522. XCR=0.497958

********** CHF CORRELATIONS **********

	XCR	XCISE	XCISM	XAI	XWES	XGE1	XGE2	XGE3	XGE4	XDOR
	0.498	0.518	0.423	0.565	0.469	0.436	0.462	0.465	0.474	0.573
% D-EXP =		4.06	-15.02	13.44	-5.86	-12.49	-7.32	-6.56	-4.89	15.09
% D-COR =		3.91	-17.67	11.85	-6.23	-14.27	-7.90	-7.02	-5.14	13.11

QCRIT FOR XEXP FROM DOROSCHUK IS 573454.
QCRIT FOR XDOR FROM DOROSCHUK IS 495515.

Figure 4c.

CORRELATING DATA #1--DNB EFFECTS TEST PROG "THAN"
20.3 10 FEB 77 1230 PL20-3A

LOCAT (FT)	HEAT TRANSF COEF (BTU/HR.SQFT.F) NA(OD)	WALL	H2O	U	SLIP RATIO	PRESS DROP (PSI) FRICT	ACCE	GRAV	TWO PHASE MULT	SPECIFIC VOL (CUFT/LBM) HOMOG	GRAV	ACCEL
-0.75	0.	0.	0.	0.	1.000	0.	0.	0.	1.00	0.02156	0.02156	0.02156
0.50	4529.	3082.	-43772.	2260.	1.000	0.44	0.	0.40	1.00	0.02155	0.02155	0.02155
1.50	4520.	3078.	-43365.	2257.	1.000	0.54	0.00	0.72	1.00	0.02172	0.02172	0.02172
1.641			********NUCLEATE BOILING********									
1.64	4519.	3078.	-37572.	2275.	1.135	0.56	0.00	0.77	1.14	0.02174	0.02177	0.02177
2.50	4511.	3075.	56923.	2065.	1.167	0.67	0.07	1.00	1.35	0.02563	0.02508	0.02508
3.50	4501.	3073.	27047.	1983.	1.210	0.83	0.14	1.24	1.63	0.03069	0.02916	0.02919
4.50	4489.	3071.	27815.	1985.	1.261	1.03	0.23	1.44	1.98	0.03661	0.03362	0.03369
5.50	4475.	3069.	36603.	2017.	1.321	1.26	0.33	1.62	2.42	0.04371	0.03859	0.03875
6.50	4457.	3067.	53935.	2050.	1.394	1.55	0.43	1.78	2.96	0.05231	0.04415	0.04449
7.50	4437.	3064.	78227.	2070.	1.482	1.91	0.56	1.92	3.65	0.06273	0.05032	0.05104
8.00	4425.	3062.	78298.	2068.	1.533	2.11	0.63	1.98	4.05	0.06874	0.05367	0.05469
8.50	4412.	3060.	63538.	2052.	1.589	2.33	0.70	2.04	4.49	0.07526	0.05715	0.05857
9.00	4398.	3057.	48510.	2029.	1.648	2.57	0.78	2.10	4.98	0.08231	0.06076	0.06272
9.25	4391.	3055.	40441.	2010.	1.680	2.70	0.82	2.13	5.24	0.08607	0.06263	0.06493
9.50	4383.	3053.	32045.	1983.	1.713	2.83	0.86	2.16	5.50	0.08993	0.06452	0.06719
9.75	4375.	3051.	25710.	1951.	1.746	2.97	0.91	2.18	5.77	0.09389	0.06643	0.06951
10.00	4367.	3049.	22047.	1925.	1.781	3.12	0.95	2.21	6.05	0.09797	0.06835	0.07191
10.17	4362.	3048.	20704.	1913.	1.805	3.22	0.99	2.22	6.25	0.10077	0.06966	0.07357
10.33	4356.	3047.	20117.	1907.	1.829	3.33	1.02	2.24	6.45	0.10363	0.07098	0.07526
10.50	4351.	3046.	20184.	1906.	1.854	3.44	1.05	2.26	6.67	0.10656	0.07233	0.07701
10.67	4345.	3045.	20644.	1909.	1.879	3.55	1.09	2.27	6.89	0.10957	0.07370	0.07882
10.83	4339.	3044.	21522.	1915.	1.906	3.67	1.12	2.29	7.13	0.11268	0.07510	0.08070
11.00	4332.	3043.	23042.	1926.	1.933	3.79	1.16	2.30	7.38	0.11589	0.07654	0.08266
11.17	4326.	3042.	25226.	1938.	1.961	3.91	1.20	2.32	7.65	0.11922	0.07802	0.08470
11.33	4319.	3042.	27954.	1952.	1.990	4.04	1.24	2.33	7.92	0.12266	0.07955	0.08684
11.50	4312.	3041.	31178.	1965.	2.020	4.17	1.28	2.35	8.21	0.12623	0.08112	0.08907
11.67	4305.	3040.	35069.	1977.	2.052	4.31	1.32	2.36	8.51	0.12993	0.08274	0.09142
11.83	4297.	3040.	39821.	1990.	2.084	4.46	1.37	2.37	8.83	0.13376	0.08441	0.09388
12.00	4290.	3039.	45715.	2001.	2.118	4.60	1.42	2.39	9.16	0.13773	0.08614	0.09647
12.33	4274.	3037.	63344.	2023.	2.188	4.93	1.52	2.41	9.86	0.14605	0.08977	0.10202
12.50	4265.	3036.	75685.	2032.	2.226	5.09	1.58	2.43	10.24	0.15050	0.09170	0.10505
12.67	4256.	3035.	93575.	2040.	2.264	5.27	1.64	2.44	10.64	0.15506	0.09369	0.10822
12.83	4247.	3034.	119858.	2048.	2.304	5.45	1.71	2.45	11.05	0.15978	0.09576	0.11156
13.00	4238.	3033.	161769.	2055.	2.346	5.63	1.77	2.46	11.48	0.16467	0.09791	0.11509
13.17	4228.	3032.	238117.	2062.	2.388	5.83	1.84	2.47	11.92	0.16972	0.10015	0.11880
13.33	4218.	3031.	417507.	2067.	2.433	6.03	1.92	2.49	12.39	0.17495	0.10249	0.12273
13.50	4207.	3030.	453306.	2072.	2.478	6.24	2.00	2.50	12.88	0.18035	0.10493	0.12688
13.67	4197.	3028.	468225.	2076.	2.525	6.46	2.08	2.51	13.38	0.18594	0.10748	0.13126
13.83	4186.	3027.	483485.	2079.	2.574	6.68	2.17	2.52	13.91	0.19171	0.11016	0.13590
14.00	4174.	3025.	319851.	2082.	2.625	6.92	2.26	2.53	14.46	0.19768	0.11297	0.14080
14.17	4163.	3024.	243570.	2084.	2.677	7.16	2.36	2.54	15.04	0.20384	0.11593	0.14598
14.33	4150.	3022.	202670.	2084.	2.730	7.42	2.46	2.55	15.64	0.21020	0.11905	0.15146
14.50	4138.	3020.	177992.	2085.	2.786	7.68	2.57	2.56	16.26	0.21676	0.12234	0.15727
14.75	4119.	3018.	154872.	2084.	2.872	8.10	2.75	2.57	17.24	0.22695	0.12764	0.16658
14.75	4120.	3018.	134916.	2088.	2.868	8.10	2.74	2.57	17.21	0.22657	0.12741	0.16617
14.750			********FILM BOILING********									
14.75	4120.	2925.	942.	641.	2.868	8.10	2.74	2.57	17.21	0.22657	0.12741	0.16617
15.00	4114.	2922.	923.	633.	2.891	8.44	2.79	2.58	13.73	0.22919	0.12881	0.16863
15.25	4108.	2920.	902.	622.	2.918	8.78	2.84	2.60	13.78	0.23246	0.13056	0.17170
15.50	4102.	2917.	882.	612.	2.946	9.11	2.90	2.61	13.84	0.23573	0.13234	0.17479
16.00	4092.	2871.	19.	19.	2.990	9.79	3.00	2.64	13.95	0.24102	0.13529	0.17990

Figure 4d.

CORRELATING DATA #2--DNB EFFECTS TEST PROG "THAN
20 3 10 FEB 77 1230 PL20-3A

LOCAT (FT)	*CORRELATION RATIOS (CORR/EXP) #1	#2	#3	#4	#5	REYNOLDS NUMBER
0.500	-0.07	-0.07	-0.07	-0.18	-7.47	0.1549E 06
1.500	-0.07	-0.07	-0.07	-0.18	-7.88	0.1566E 06
1.641	********NUCLEATE BOILING********					
1.641	-0.21	0.	0.	0.	1.90	0.1568E 06
2.500	0.14	0.	0.	0.	1.48	0.1568E 06
3.500	0.32	0.	0.	0.	1.32	0.1568E 06
4.500	0.34	0.	0.	0.	1.27	0.1568E 06
5.500	0.28	0.	0.	0.	1.27	0.1568E 06
6.500	0.21	0.	0.	0.	1.27	0.1567E 06
7.500	0.16	0.	0.	0.	1.26	0.1567E 06
8.000	0.17	0.	0.	0.	1.24	0.1567E 06
8.500	0.22	0.	0.	0.	1.21	0.1567E 06
9.000	0.29	0.	0.	0.	1.18	0.1567E 06
9.250	0.36	0.	0.	0.	1.16	0.1566E 06
9.500	0.46	0.	0.	0.	1.13	0.1566E 06
9.750	0.58	0.	0.	0.	1.09	0.1566E 06
10.000	0.69	0.	0.	0.	1.07	0.1566E 06
10.167	0.74	0.	0.	0.	1.06	0.1566E 06
10.333	0.77	0.	0.	0.	1.05	0.1566E 06
10.500	0.78	0.	0.	0.	1.05	0.1566E 06
10.667	0.77	0.	0.	0.	1.05	0.1566E 06
10.833	0.75	0.	0.	0.	1.05	0.1566E 06
11.000	0.71	0.	0.	0.	1.06	0.1566E 06
11.167	0.66	0.	0.	0.	1.07	0.1566E 06
11.333	0.61	0.	0.	0.	1.08	0.1566E 06
11.500	0.56	0.	0.	0.	1.08	0.1566E 06
11.667	0.50	0.	0.	0.	1.09	0.1566E 06
11.833	0.45	0.	0.	0.	1.10	0.1566E 06
12.000	0.40	0.	0.	0.	1.11	0.1565E 06
12.333	0.30	0.	0.	0.	1.13	0.1565E 06
12.500	0.25	0.	0.	0.	1.13	0.1565E 06
12.667	0.21	0.	0.	0.	1.14	0.1565E 06
12.833	0.17	0.	0.	0.	1.15	0.1565E 06
13.000	0.12	0.	0.	0.	1.15	0.1565E 06
13.167	0.09	0.	0.	0.	1.16	0.1565E 06
13.333	0.05	0.	0.	0.	1.16	0.1565E 06
13.500	0.05	0.	0.	0.	1.16	0.1565E 06
13.667	0.05	0.	0.	0.	1.17	0.1564E 06
13.833	0.05	0.	0.	0.	1.17	0.1564E 06
14.000	-0.07	0.	0.	0.	1.17	0.1564E 06
14.167	-0.09	0.	0.	0.	1.17	0.1564E 06
14.333	-0.11	0.	0.	0.	1.17	0.1564E 06
14.500	-0.13	0.	0.	0.	1.17	0.1564E 06
14.750	-0.15	0.	0.	0.	1.17	0.1564E 06
14.750	-0.18	0.	0.	0.	1.18	0.1563E 06
14.750	********FILM BOILING********					
14.750	0.53	1.86	1.65	0.	-0.55	0.6557E 06
15.000	0.54	1.88	1.70	0.	-0.58	0.6542E 06
15.250	0.55	1.91	1.75	0.	-0.61	0.6524E 06
15.500	0.56	1.93	1.81	0.	-0.64	0.6506E 06

MEAN RATIOS	#1	#2	#3	#4	#5
COOLED	-0.067	-0.071	-0.071	-0.180	-7.675
NUCLEATE	0.317	0.	0.	0.	1.153
FILM	0.551	1.907	1.752	0.	-0.610

Figure 4e.

$$T_N = T_s - \frac{q''}{h_N} \frac{D_i}{D_o} \left(\frac{h_N}{BK_{eff}} - 1 \right) \beta \qquad (1)$$

Here, h_N is the sodium heat transfer coefficient, determined from Dwyer's equations for the inside surface of an annulus.[7,8] The parameter K_{eff} is an effective sodium thermal conductivity to account for both molecular and eddy conduction after Dwyer.[7] The parameter B is determined from the following analytical relationship:[3]

$$B = \frac{4(D_s^2 - D_o^2)}{2D_o D_s^2 \ln \frac{D_s}{D_o} - D_o(D_s^2 - D_o^2)} \qquad (2)$$

The parameter β in Equation (1) is a spacer adjustment factor intended to account for mixing downstream of the tube spacers and the entrance region. The mixing is believed to increase stream turbulence near the shell-side of the annulus and, consequently, increases the actual shell-side sodium heat transfer coefficient. This mixing causes the slope of the shell temperatures to differ drastically from that of the corresponding bulk sodium temperatures. Because of this, the determination of the CHF location and heat flux curve are very difficult without first determining the bulk sodium temperatures, and the calculation of the bulk sodium temperatures are dependent upon the β factors. The β-values vary between 0.0 and 1.0, depending upon the axial distance from the spacer with no variation between tests. Not varying the β-values between tests results in only relatively small errors.

Another relationship between the bulk sodium temperature and the heat flux is:

$$q'' = \frac{W_N C_N}{\pi D_i} \frac{dT_N}{dZ} \qquad (3)$$

Iteration with Equations (1) and (3) results in T_N for each of the axial measurement stations.

Two separate and distinct processes of CHF have been observed, namely, departure from nucleate boiling (DNB) and dryout.[9-11] Since all of the current data fall into the annular flow regime associated with liquid film dryout-type CHF, an abrupt change in q" at the CHF point was adopted for treating the current data. An abrupt change in q" follows the recommendation for treating dryout, as opposed to a smooth change for DNB-type CHF, adopted by other research engineers.[2] The CHF point is located by first fitting the bulk

sodium temperature with a smooth fourth-order spline curve, based on sets of 10 sequential points. Selective trial methods have shown that the intersection of two separate split curves, as required to represent an abrupt change in q" at CHF, corresponds very closely to the axial location of the minimum second derivative of the smooth curve representing T_N. Consequently, the CHF point was located at the axial position corresponding to the minimum second derivative. The bulk sodium temperature points were then fitted with two separate curves, split at the CHF point to replace the initial smooth curve. The final bulk sodium temperature points, before CHF, were fitted with a fourth-order spline curve based on sets of 10 points, and after CHF, were fitted with a low-order, least-square curve fit. A final heat-flux curve is determined from the split sodium temperature curves by using Equation (3). The CHF point occurs at the maximum heat flux as shown in Figure 4a.

The refinement in the data evaluation achieved by including the effect of radial sodium temperature distribution in the analysis results in the CHF point generally calculated to be several inches downstream (relative to the water flow) of the location predicted based on the assumption that the sodium bulk temperature gradient is equal to the shell temperature gradient. A different technique, employed by ANL to account for the same phenomenon, resulted in similar relative predictions.[12] These predictions have been confirmed during tests conducted by ANL in the SGTF, by observing that the predicted CHF location corresponds to the axial location of an internal thermocouple, embedded in the tube wall, which was recording oscillations in the transition boiling region.

Other temperature distributions, shown in Figure 4a, of the outside and inside tube wall and the bulk water, and steam quality at CHF are determined from a heat balance repeated in step-wise fashion along the test section.

5. RESULTS

5.1 CHF CORRELATION

The CHF test results at 7.2 MPa nominal pressure have been divided into two groups, namely, for high- and low-mass flux regions and are summarized in Appendix A, Tables A-1 and A-2, respectively. These regions are intended to be representative of nominal LMFBR operating conditions for the high-mass flux region and severely partially plugged steam

generator tube conditions for the low-mass flux region. The CHF results for these regions are separately discussed in the following two subsections.

5.1.1 CHF for High-Mass Flux

The experimental ranges of the high-mass flux CHF data are:

• pressure, P_c	7.2 MPa	(1040 psia)
• mass flux, G	540-1490 kg/s.m^2	(0.40-1.10 10^6 lbm/h·ft^2)
• critical heat flux, q''_c	0.69-1.86 MW/m^2	(0.22-0.59 10^6 Btu/h·ft^2)
• critical steam quality, X_c	0.48-0.89	

A typical computer-generated plot for each high-mass flux test series is presented in Appendix B, Figures B-1 through B-10. All the experimental CHF results, as summarized in Table A-1, are presented in Figures 5 and 6. Figure 5 shows that the critical steam quality, X_c, for fixed pressure and mass flux for the range of test conditions is independent of heat flux, q''_c. Figure 6 shows that the critical steam quality decreases rapidly with mass flux for fixed pressure.

The critical steam quality data are compared in Figures 7a-d with other known correlations which come quite close to the range of parameters investigated in the current study. In Figures 7a and 7b the experimental X_c-values are compared with X_c-values predicted with the CISE[13] and Doroschuk[11] correlations, respectively. Both of these correlations are based on data obtained from electrical-heated test sections. In Figures 7c and 7d similar comparison is made with the recent Westinghouse-Hwang[1] and GE[2] correlations, respectively, based on data obtained from sodium-heated test sections. The relative standard deviations of the data comparisons are as follows:

	σ(%)
CISE[13]	7.2
Doroschuk[11]	9.9
Westinghouse-Hwang[1]	7.2
GE - 1976[2]	8.2

Thus, any of the above correlations could be used to predict critical quality over the experimental ranges with uncertainties up to about 20% at a 95% probability level.

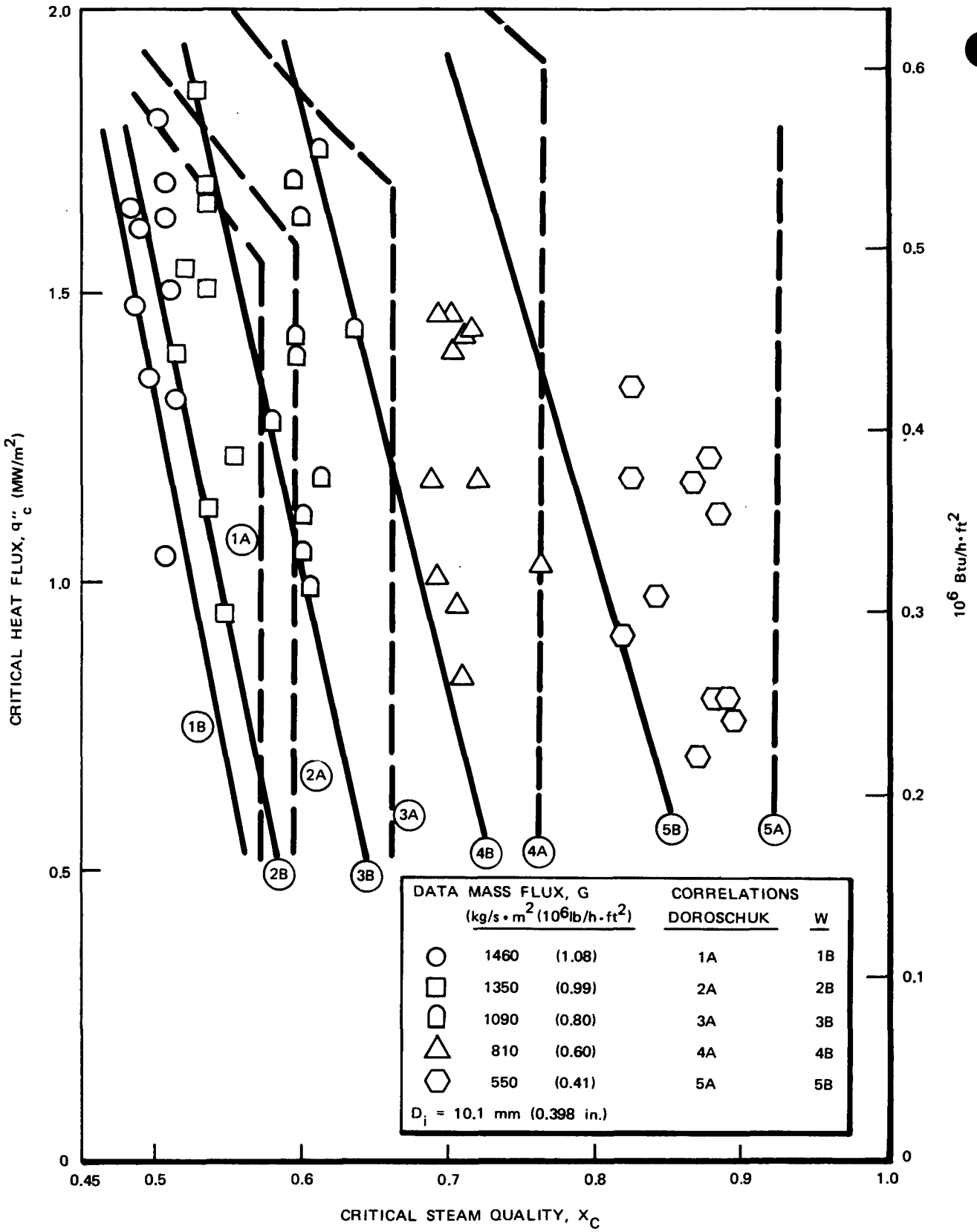

Figure 5. Critical Heat Flux versus Critical Steam Quality for High Mass Flux at P_C = 7.2 MPa (1040 psia)

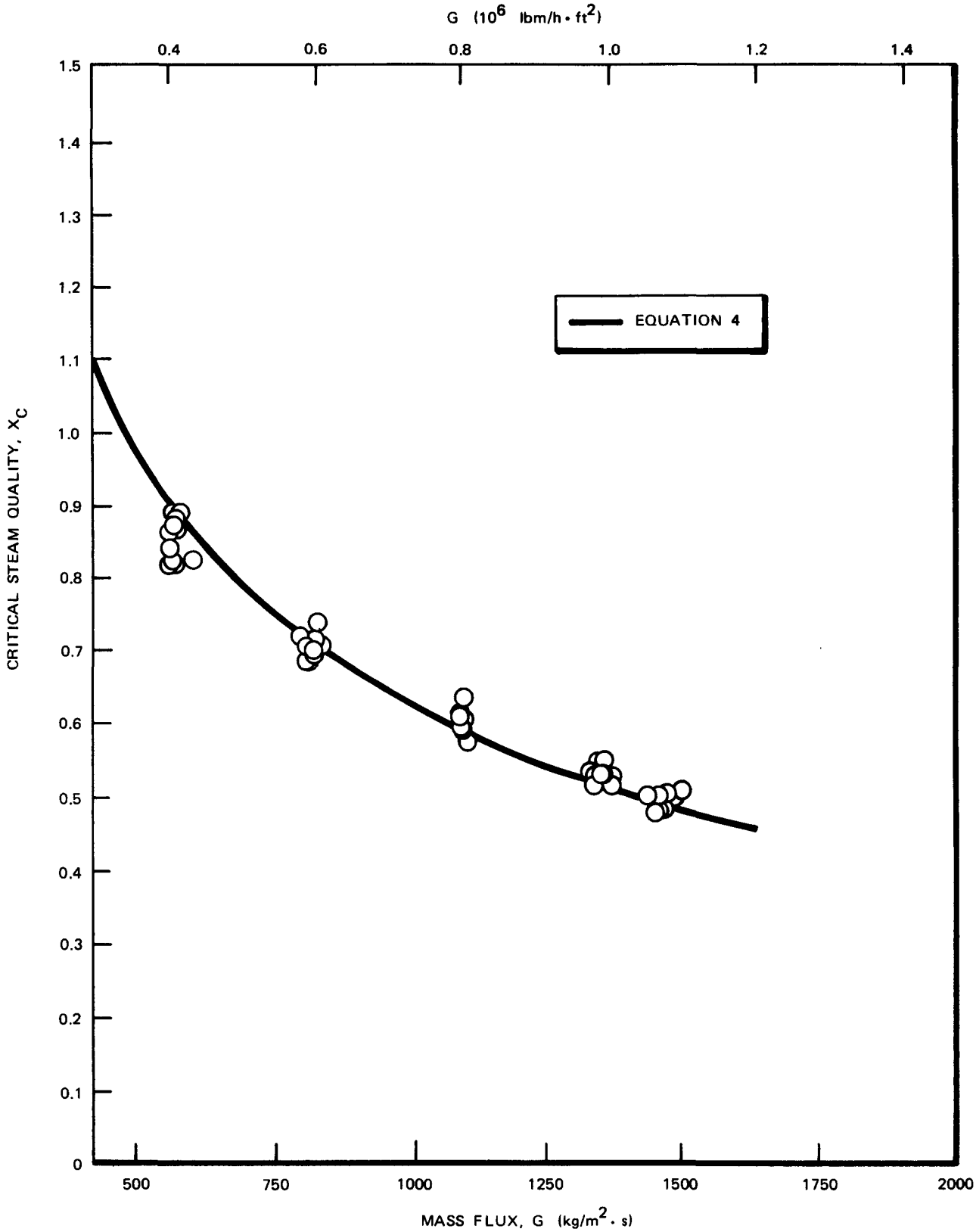

Figure 6. Critical Steam Quality versus Mass Flux at P_C = 7.2 MPa

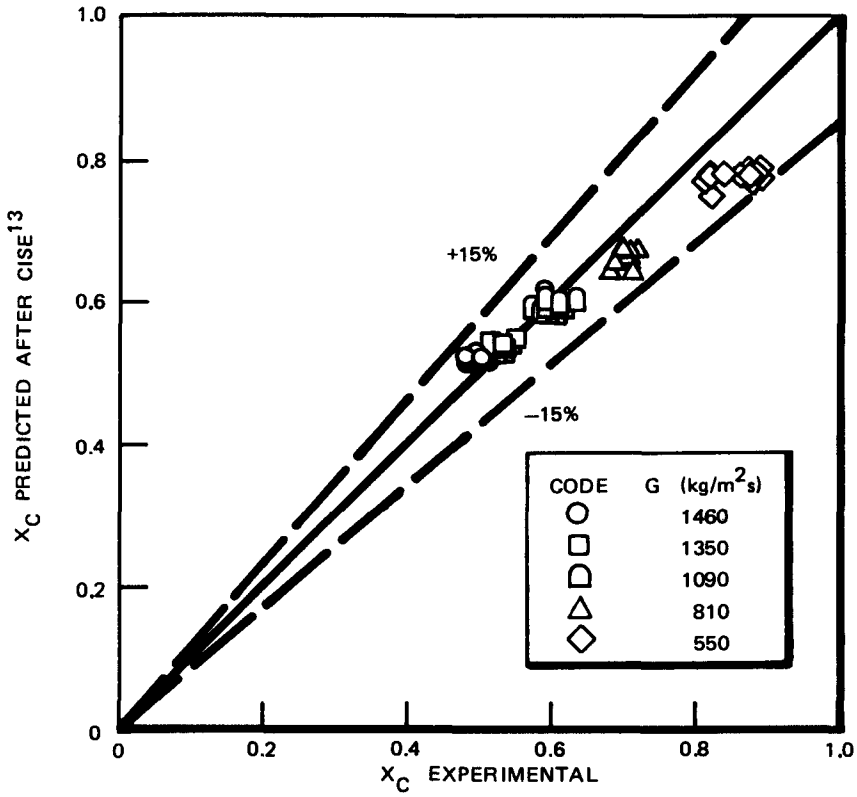

Figure 7a. CISE Correlation

Figure 7. Comparison of Experimental Critical Steam Quality for High Mass Flux at P_C = 7.2 MPa with Predictions

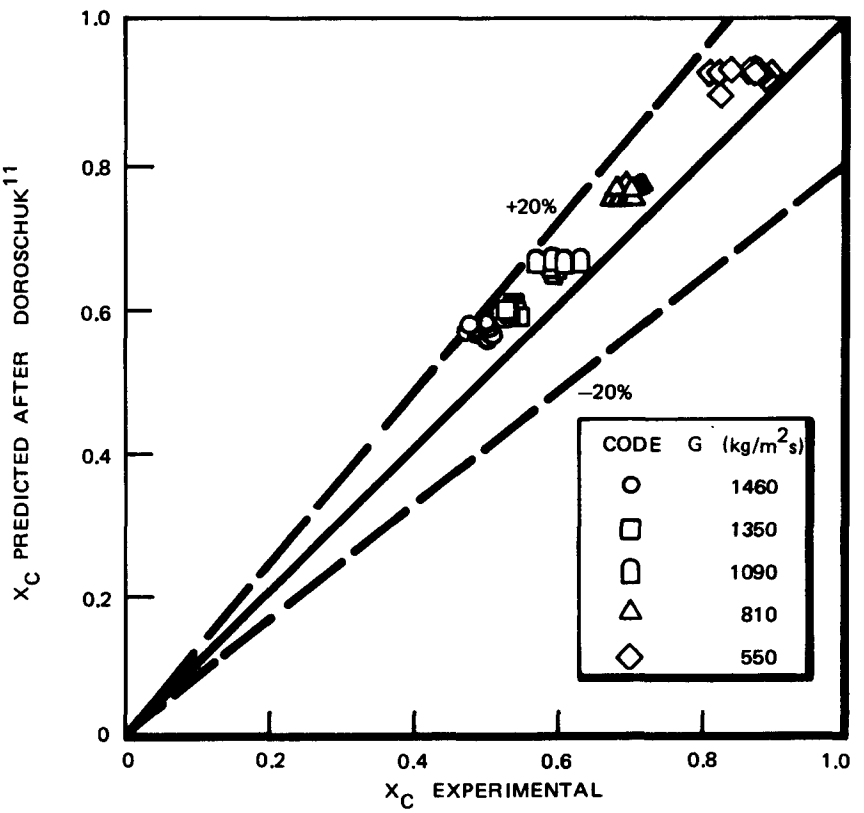

Figure 7b. Doroschuk Correlation

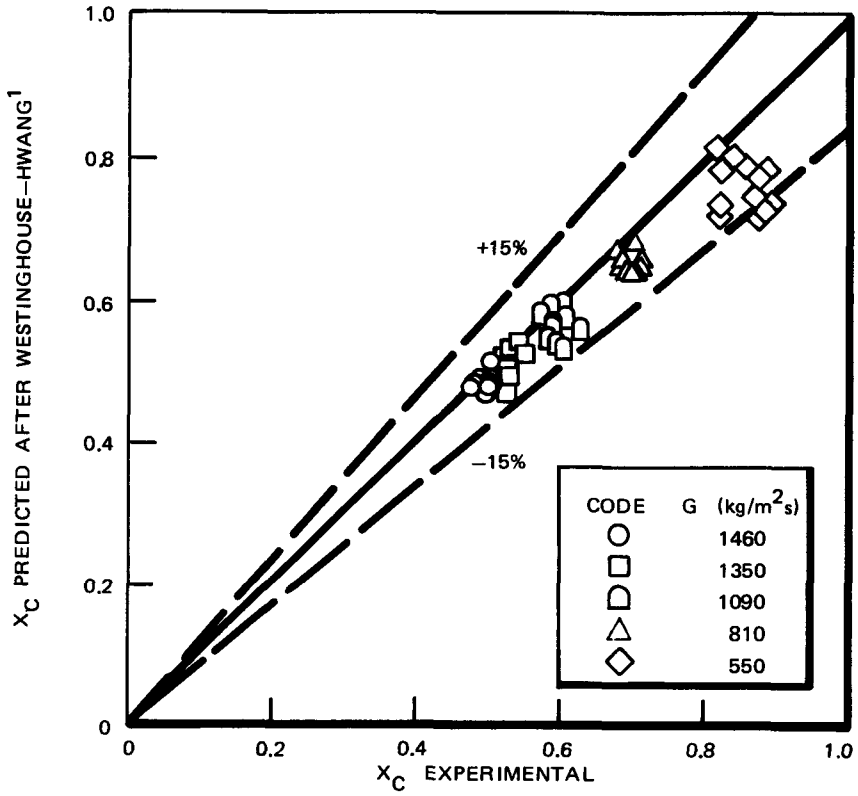

Figure 7c. Westinghouse – Hwang Correlation

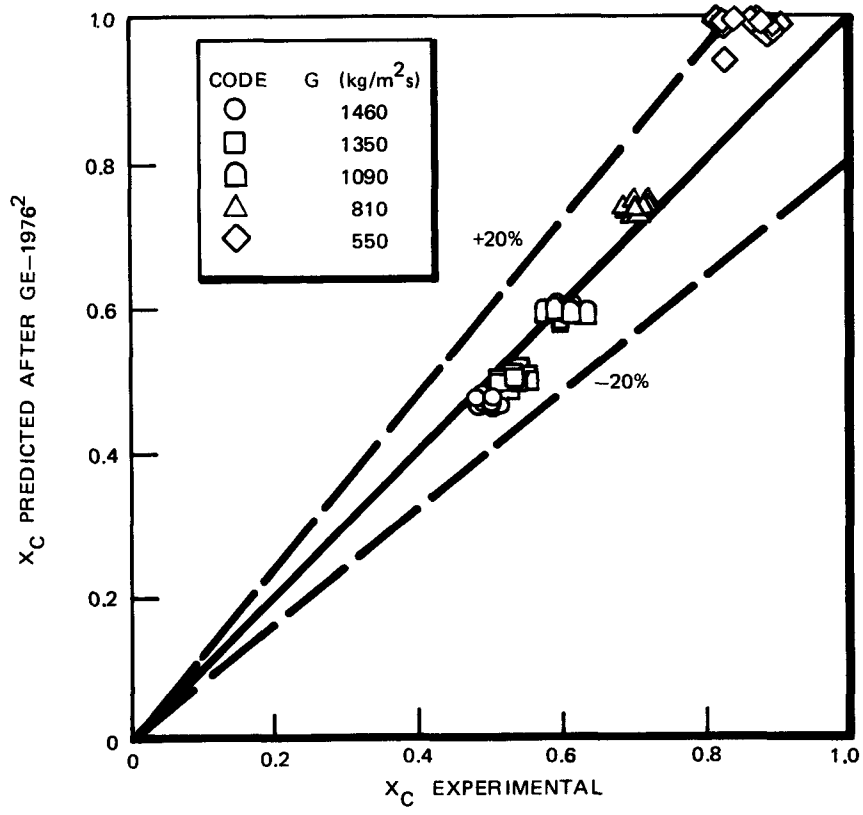

Figure 7d. GE–1976 Correlation

The Doroschuk[11] and Westinghouse[1] correlations are further compared with the data in Figure 5. Figure 5 shows that the Westinghouse correlation generally underpredicts the critical quality data, while the Doroschuk correlation overpredicts. The data show, contrary to the Westinghouse correlation,[1] that critical quality is independent of the critical heat flux. The trend of the data confirms that the CHF phenomenon is of the dryout type as opposed to DNB. The Doroschuk[11] correlation consists of two parts, one for dryout and another for DNB. The dryout portion has X_C independent of heat flux as demonstrated with the current data. The previous GE data[2] obtained mostly at higher pressures up to 13 MPa also demonstrated that X_c is independent of heat flux over the experimental ranges.

A simpler and more accurate critical steam quality correlation than the previously referenced correlations was fitted to the GE sodium-heated CHF data obtained during the current and previous[2] investigations. The derived empirical correlation is[a]:

$$X_c = \frac{0.944\ (1 - P_{c,r})^{1.054}}{(G/10^3)^{0.625}} \qquad (4)$$

The data are compared with predictions with Equation (4) in Figure 8. The relative standard deviation is 4.7% for all the GE data and 3.8% for the current data at a nominal pressure of 7.2 MPa. The experimental ranges of the data supporting the correlation are:

P_c = 7.0-13.0 MPa	(1015-1890 psia)
G = 540-3250 kg/s·m^2	(0.40-2.40 10^6 lbm/h·ft^2)
q''_c = 0.69-1.86 MW/m^2	(0.22-0.59 10^6 Btu/h·ft^2)
D_i = 10.1 mm	(0.398 in.)

Figure 9 presents a comparison of the X_c predictions and the Equation (4) correlation with other dryout-type CHF data obtained from a sodium-heated steam generator test, with a 10.0 mm (0.394 in.) inside diameter tube conducted at ANL,[14,15] at conditions encompassed by the GE data. The agreement between the ANL-inferred dryout data and Equation (4) predictions is very good.

---

[a] In U.S. customary units: $X_c = \frac{0.780\ (1 - P_{c,r})^{1.054}}{(G/10^6)^{0.625}}$ for G in lbm/h ft^2.

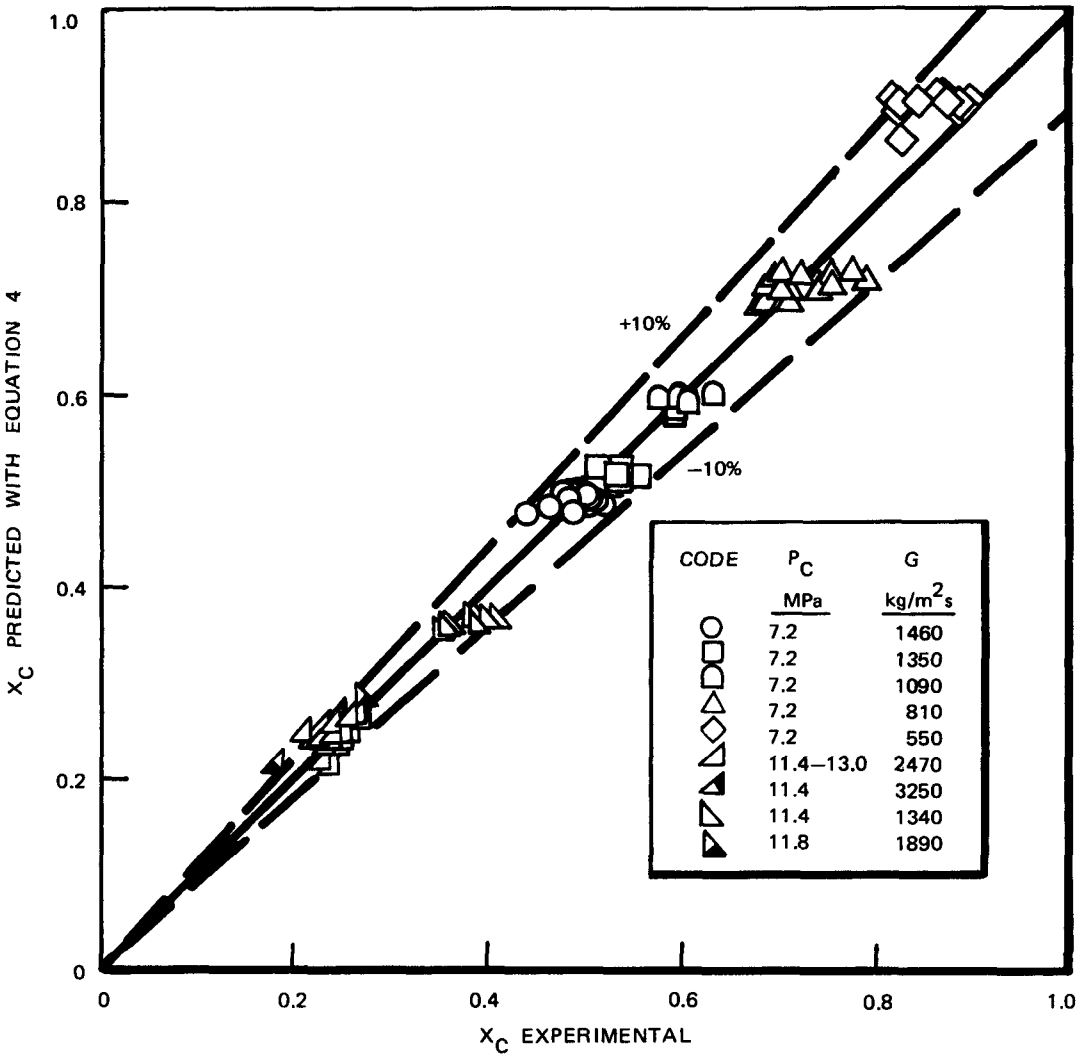

Figure 8. Comparison of GE Critical Quality Data with Correlation, Equation 4

The relative standard deviation of ANL data alone is 8.3% and when combined with the GE data, 5.8%. Further agreement between the GE data and ANL data is illustrated in Figure 10 for conditions selected to approximate the GE proposed PLBR conditions.

Equation (4) is currently recommended for dryout-type CHF, as opposed to DNB for the ranges of experimental parameters previously given and for relatively long tubes with an inside diameter corresponding to the test tube, 10.1 mm (0.398 in.), heated by sodium flowing in the countercurrent direction. The critical steam quality in tubes of other diameters can be determined by adjusting the X_C-value calculated from Equation (4) according to the effect predicted by other correlations as discussed later.

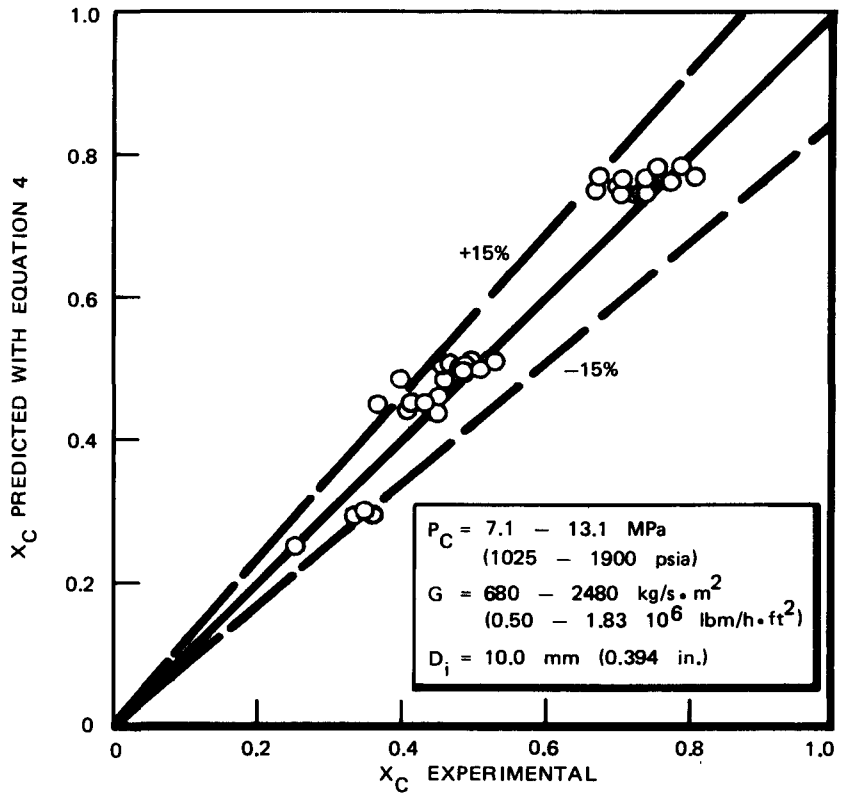

Figure 9. Comparison of ANL Critical Steam Quality Data with Correlation, Equation 4

Additional experimental work is currently in progress to increase the data base and extend the ranges of parameters affecting CHF for sodium-heated conditions. These latter test results along with the current results and other recently published sodium-heated CHF results should provide the basis for an even more general CHF correlation for sodium-heated evaporator tubes.

5.1.2 CHF for Low-Mass Flux

The experimental ranges of the low-mass flux CHF data are:

- pressure, P_C — 7.2 MPa (1050 psia)
- mass flux, G — 110-270 kg/s•m^2 (0.08-0.20 10^6 lbm/h•ft^2)
- critical heat flux, q''_C — 0.16-1.01 MW/m^2 (0.05-0.32 10^6 Btu/h•ft^2)
- critical steam quality, X_C — > 0.50

A typical computer plot for each low-mass flux test series is presented in Appendix B, Figures B-11 through B-16. All the CHF results are summarized in Table A-2 and presented in Figures 11 and 12 for nominal-mass fluxes of 260 and 130 kg/s•m^2 (0.2 and 0.1 10^6

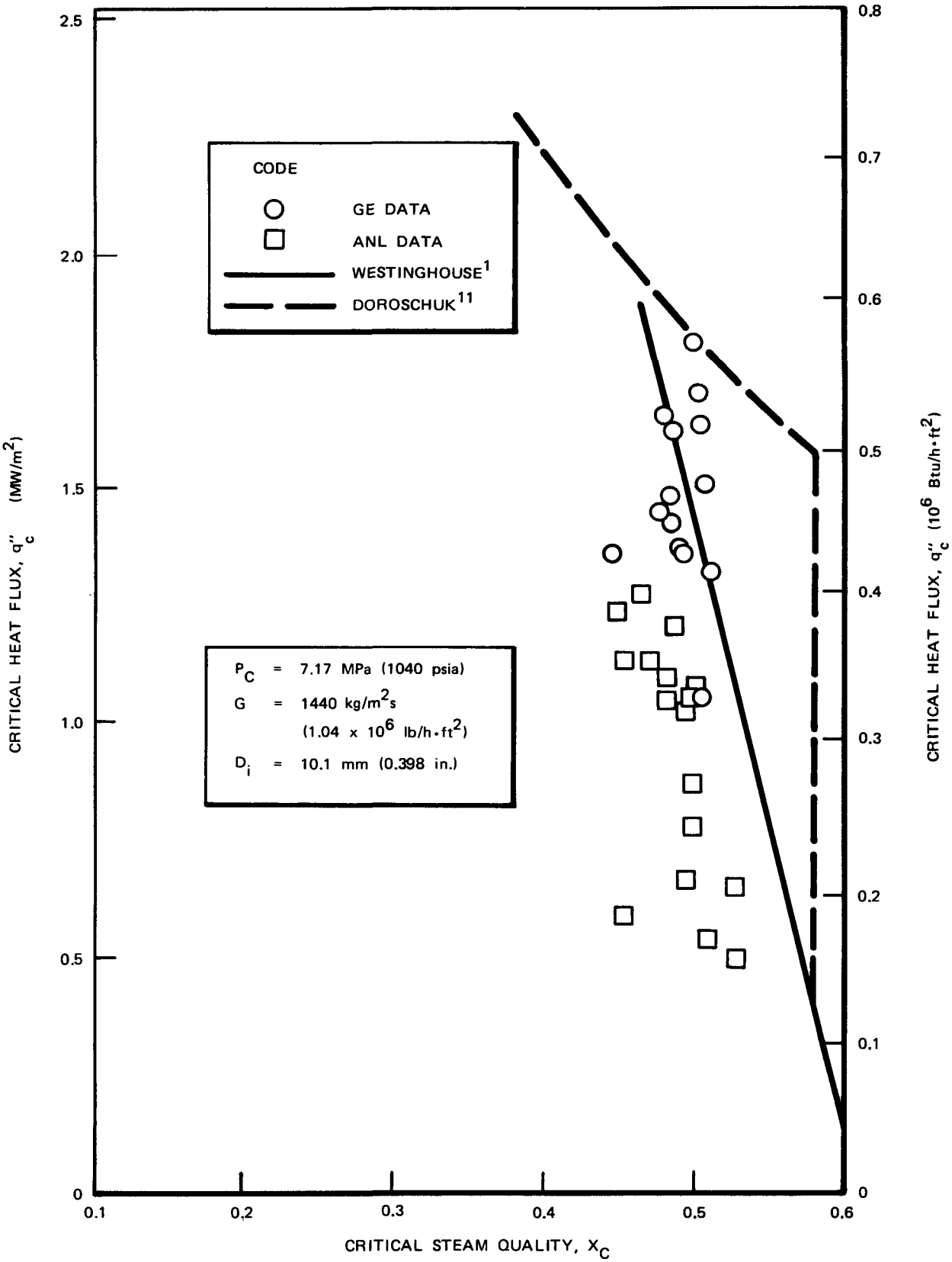

Figure 10. Comparison of GE and ANL Data for G and P_C Conditions Simulating Proposed PLBR Steam Generator Conditions

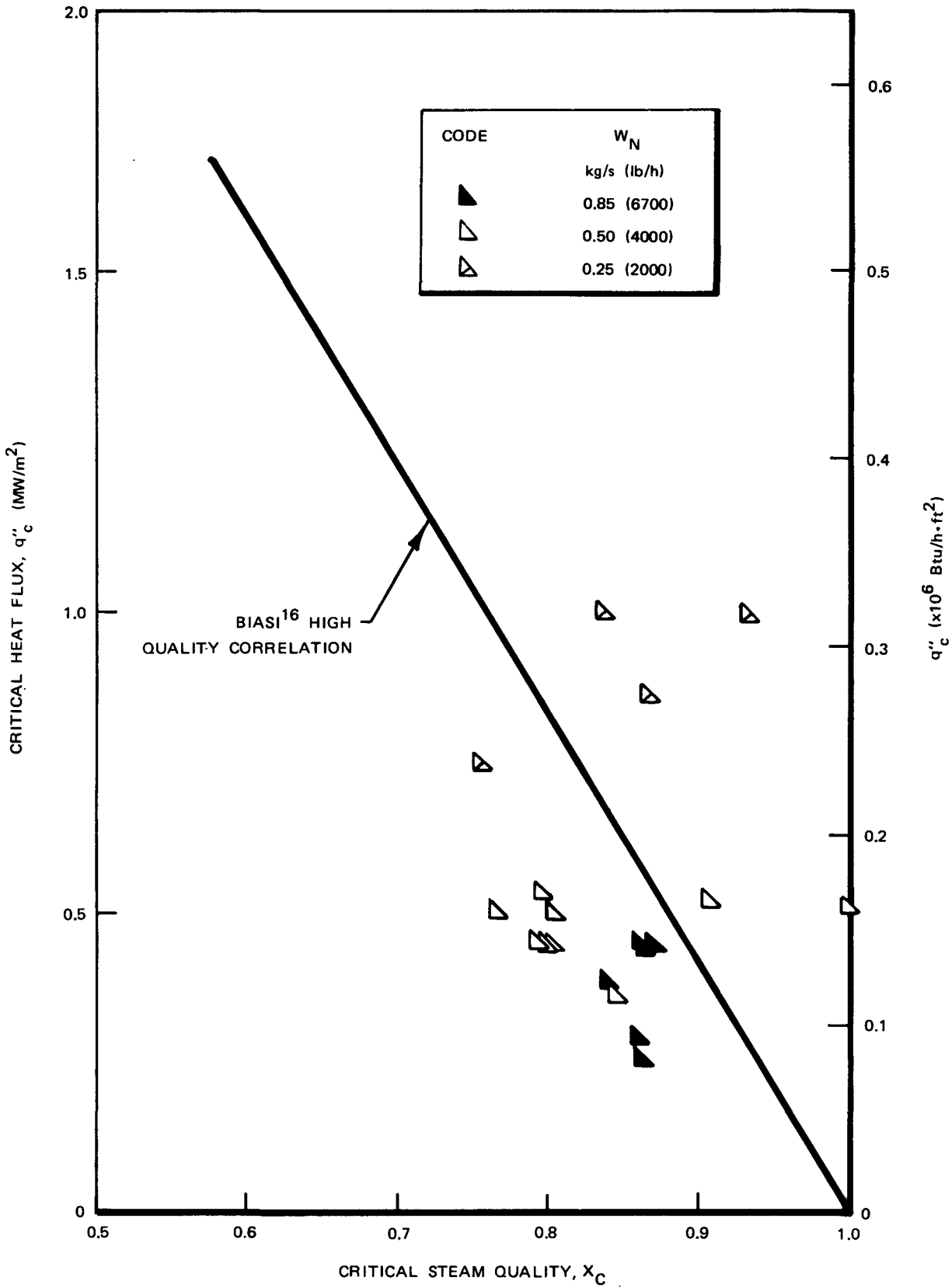

Figure 11. Critical Heat Flux versus Critical Steam Quality for G = 260 kg/s·m^2 (0.20 x 10^6 lbm/h·ft^2) and P_C = 7.2 MPa

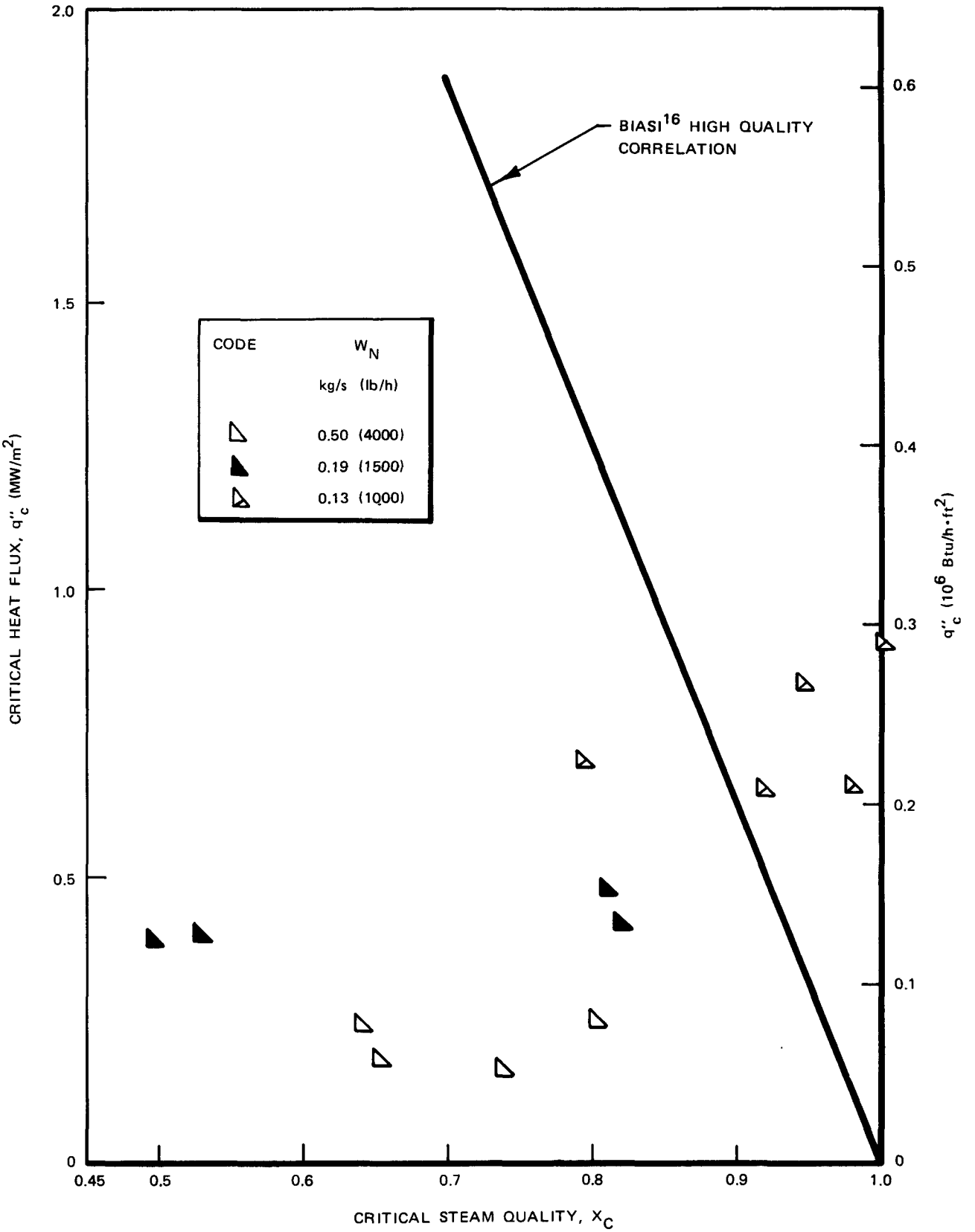

Figure 12. Critical Heat Flux versus Critical Steam Quality for G = 130 kg/s · m^2 (0.10 x 10^6 lbm/h·ft^2) and P_C = 7.2 MPa

lbm/h·ft^2), respectively. Predictions based on the correlation proposed by Biasi, et al.,[16] for the high-quality, low-mass flux region are also shown in Figures 11 and 12. For G = 260 kg/s·m^2 the data are in good agreement with the Biasi correlation. However, for G = 130 kg/s·m^2 the data show wide scatter in critical steam quality and only the high critical heat flux data having q''_c between 0.6 and 0.9 MW/m^2 show good agreement with the Biasi correlation. The scatter in X_c for G = 130 kg/s·m^2, Figure 12, exceeds the uncertainty in X_c which is estimated at a maximum of about ±0.11 for the lowest heat flux conditions. Other reasons for the wide scatter may be flow regime fluctuations with nonequilibrium conditions on the water-steam side and flow stratification on the sodium side.

5.1.3 Diameter Effect for Extrapolation to Proposed PLBR Conditions

The experimental CHF data presented apply directly to tubes with an inside diameter corresponding to the test tube, 10.1 mm (0.398 in.). For proposed PLBR conditions, the inside diameter of the steam generator tubes is 31.3 mm (1.233 in.). The diameter effect on the CHF correlation, Equation (4), must be determined to apply the current data to tubes of other diameters as for the proposed PLBR. In Figure 12, the ratio of the critical steam quality at diameter D_i to the quality at the test tube diameter of 10.1 mm is presented as a function of D_i, as predicted by several known correlations which include a diameter effect (Figure 13), for nominal proposed PLBR operating conditions. Correlations included in Figure 12 and not previously mentioned are Biasi, et al.,[16] for low quality, Kon'kov,[17] Kirby,[18] and Thompson and MacBeth.[19] The steam quality ratio, R, predicted by the Doroschuk[11] correlation is recommended for PLBR application because it is bracketed by the other correlations, agrees very well with the CISE[13] and Westinghouse[1] correlations, and is simple to apply, i.e.,

$$X_c \, D_i^{0.15} = \text{constant} \qquad (5)$$

For proposed PLBR conditions of nominal pressure and mass flux of 7.2 MPa (1040 psia) and 1490 kg/s·m^2 (1.1 x 10^6 lbm/h·ft^2), respectively, the predicted critical quality from Equation (4) is

$$X_c = 0.486 \text{ for } D_i = 10.1 \text{ mm}$$

For D_i = 31.3 mm the critical steam quality ratio, R, is 0.844 resulting in

$$X_c = 0.410 \text{ for } D_i = 31.3 \text{ mm}$$

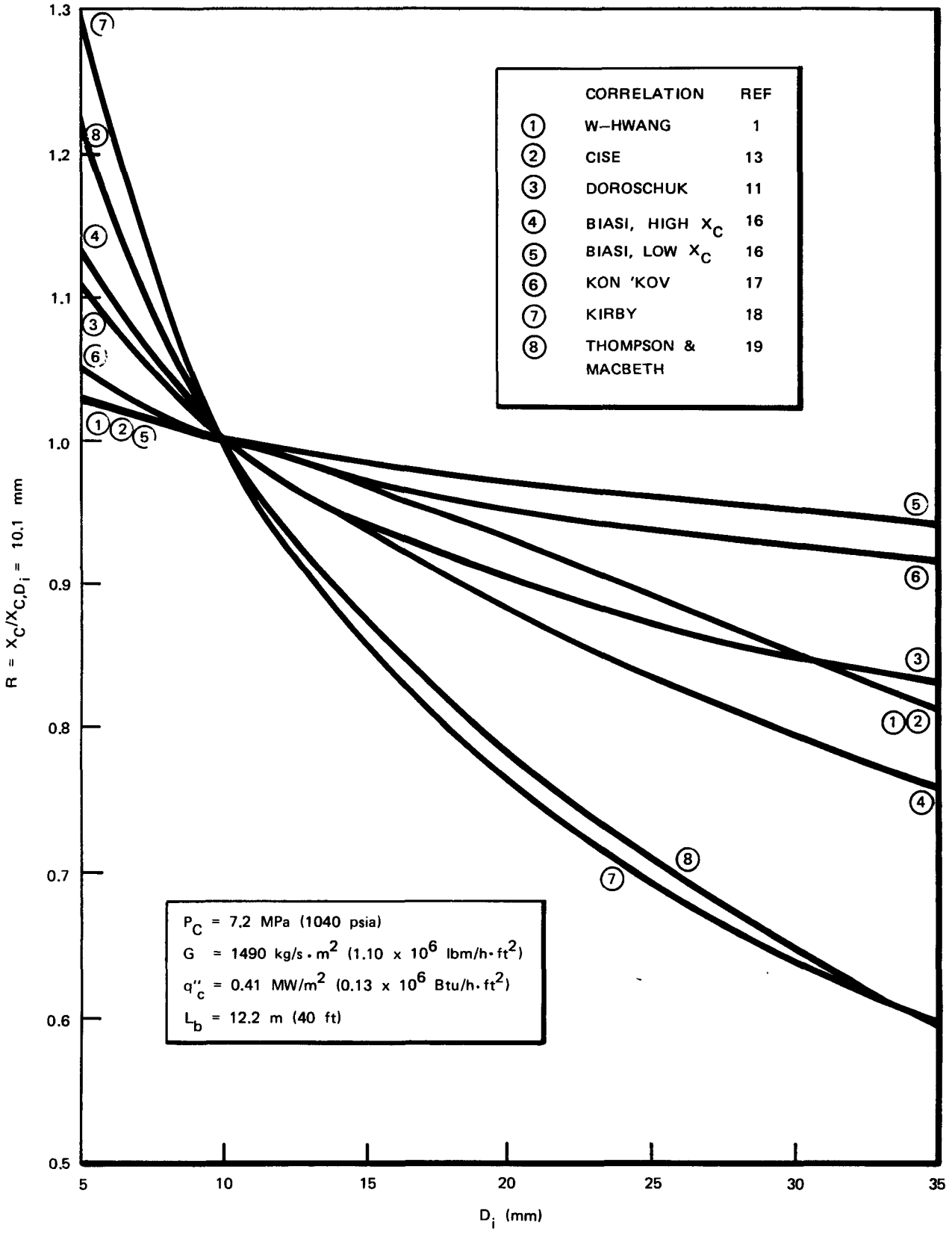

Figure 13. Effect of Diameter on Critical Steam Quality

The relative standard deviation, $\sigma_{x_{31.3}}$, of X_c for D_i = 31.3 mm can be determined from

$$\sigma_{x_{31.3}} = (\sigma_R^2 + \sigma_{x_{10.1}}^2)^{1/2} \quad (6)$$

Here σ_R and $\sigma_{x_{10.1}}$ are the relative standard deviations of R and X_c for D_i = 10.1 mm, respectively. The value of σ_R is estimated at 10% and $\sigma_{x_{10.1}}$ = 5.8% for both the GE and ANL dryout data. Hence, $\sigma_{x_{31.3}}$ = 11.6%. The discounted critical steam quality for proposed PLBR conditions is determined, based on a one-sided uncertainty with a 95% probability level as

$$X_c = 0.410 \left(1 - 1.64\sigma_{x_{31.3}}\right) = 0.33$$

5.2 TRANSITION BOILING CHARACTERISTICS

The test program also provided some information on CHF temperature oscillations and on the axial length of the region of transition from the two-phase forced convective region of heat transfer to the liquid deficient region following dryout. This was done by operating the system with the two-phase forced convective region of heat transfer extending to the tube outlet and then increasing the sodium temperature so that dryout moved into the tube and continued past the tube thermocouples A through F (see Figure 1). Figures 14 and 15 present typical tube wall temperature records for the high- and low-mass flux conditions at 7.2 MPa.

For a typical high-mass flux case with G = 1450 kg/s·m^2 (1.07 x 10^6 lbm/h·ft^2) and q''_c = 1.55 MW/m^2 (0.43 x 10^6 Btu/h·ft^2), Figure 14, thermocouples A, B, and C show temperature profiles experienced in the stable liquid deficient region. On the other hand, thermocouples D, E, and F show temperature profiles experienced first in the stable two-phase forced convective region, followed by the transition region, and finally, the stable liquid deficient region. The length, L_T, of the transition boiling region can be estimated from the temperature record and the known thermocouple spacing. If the onset of transition boiling, OTB, noted by thermocuple D, occurred at the same time as the end of the transition boiling region, ETB, noted by thermocouple F, then the transition boiling region length would be equal to the axial spacing of thermocouples D and F, i.e., 31.8 mm (1.25 in.). However, there is a time lag between OTB at location D and ETB at location F during which time the transition boiling region travels a distance ΔL. The value of ΔL can be evaluated by determining an average of the velocity for the OTB point based on its motion between locations E and D and the velocity of the ETB point based on its motion between F and E.

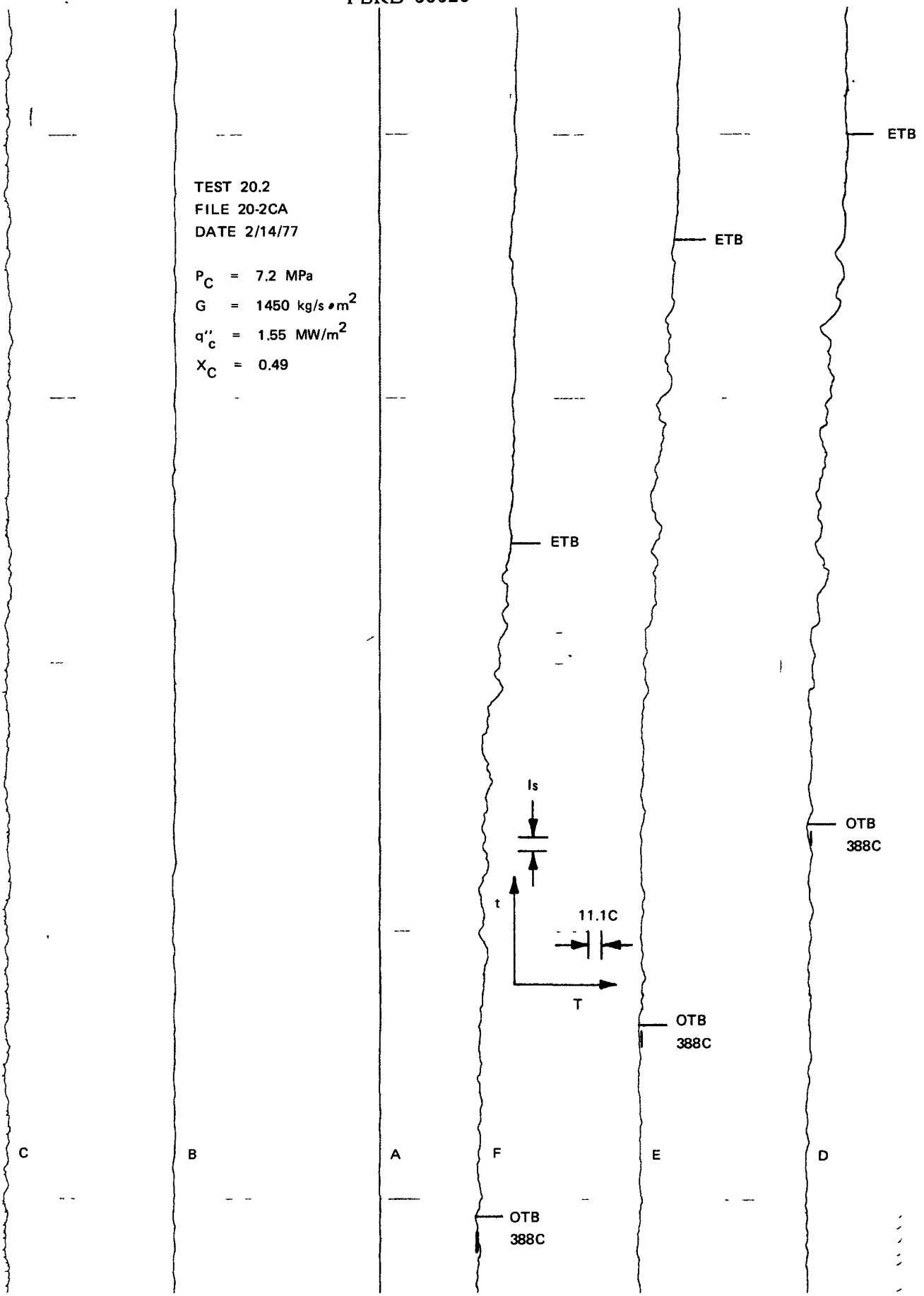

Figure 14. Tube Wall Outer Surface Temperature Behavior Near CHF for High Mass Flux

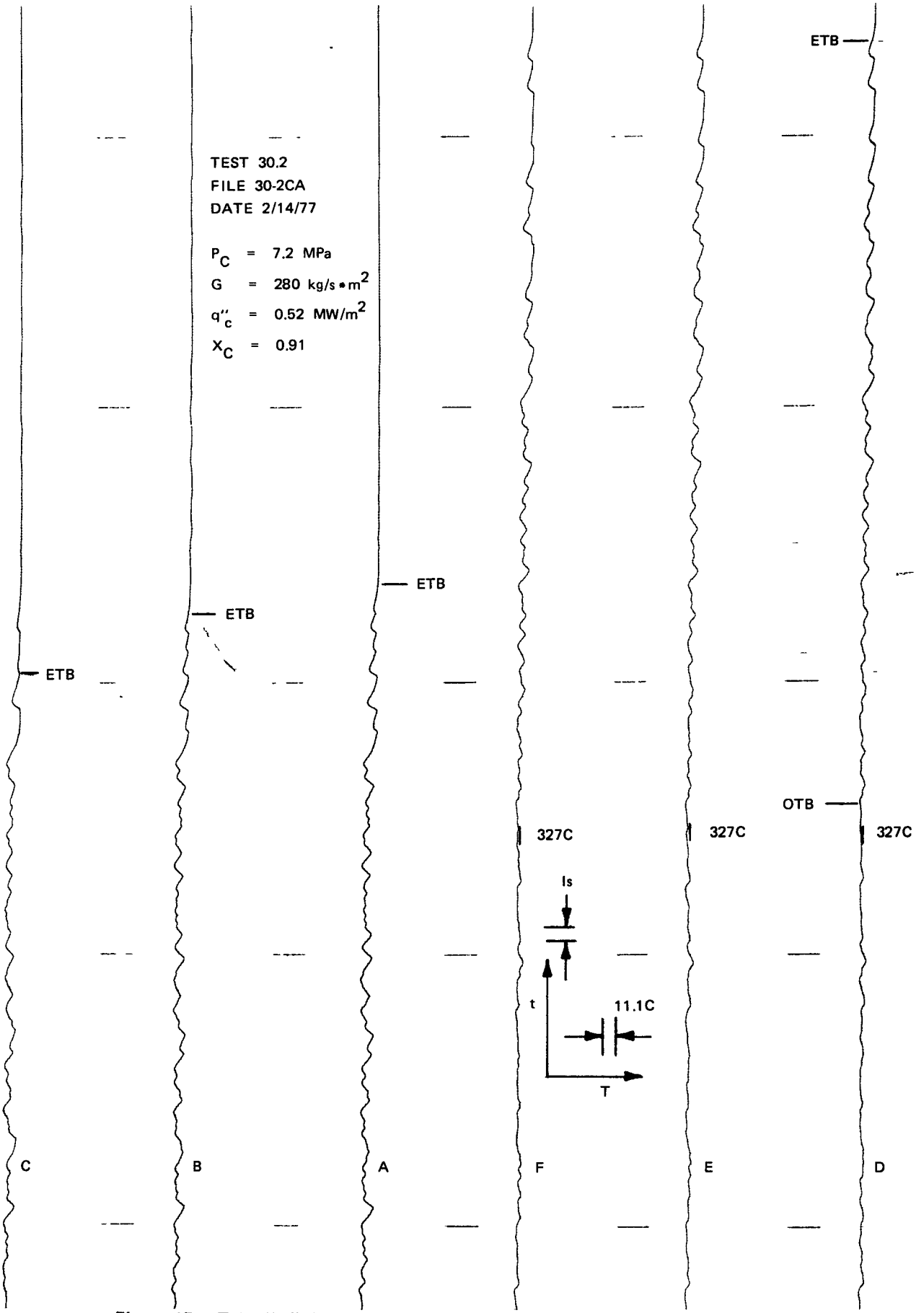

Figure 15. Tube Wall Surface Temperature Behavior Near CHF for Low Mass Flux

For the data in Figure 14, this results in L_T = 51 mm (2.0 in.). This length is in good agreement with the transition length of 41 mm (1.6 in.) previously determined for 11.0 MPa.[2]

The temperature fluctuations in the transition region for the high-mass flux case, Figure 14, show a peak-to-peak amplitude of about 14°C (25°F) and a period of about 3 seconds. The difference in thermocouple readings between OTB and ETB is about 33°C (60°F). The peak-to-peak fluctuations are, therefore, about 40% of the potential temperature difference between OTB and ETB.

For a typical low-mass flux case with G = 280 kg/s·m^2 (0.20 x 10^6 lbm/h·ft^2) and q''_c 0.52 MW/m^2 (0.17 x 10^6 Btu/h·ft^2), Figure 15, thermocouples, A, B, and C show temperature profiles in the transition region, followed by the stable liquid deficient region. Thermocouples D, E, and F show, in addition to the two regions observed with thermocouples A, B, and C, the stable two-phase forced convective region near the beginning of the traces. Here, the length, L_T, of the transition boiling region is based on the axial spacing between C and D of 184 mm (7.25 in.) and an average velocity of the ETB point between C and B, resulting in L_T = 230 mm (9.1 in.). Thus, L_T has significantly increased as the mass flux has decreased.

The temperature fluctuations in the transition region for the low-mass flux case, Figure 15, show a peak-to-peak amplitude of about 10°C (18°F) and a period of about 3 seconds. The difference in thermocouple readings between OTB and ETB is about 19°C (34°F). The peak-to-peak fluctuations are therefore about 50% of the potential temperature difference between OTB and ETB.

The transition boiling temperature fluctuations can be compared to similar fluctuations reported previously[2,3] for simulated CRBRP conditions at 11.0 MPa (1590 psia) and 2440 kg/s·m^2 (1.80 x 10^6 lbm/h·ft^2). The reported fluctuations of 14°C (25°F) for CRBRP conditions are of the same magnitude as observed for the high-mass flux case which simulates the proposed PLBR nominal G and P_c conditions with a much higher heat flux of 1.55 MW/m^2 (0.43 x 10^6 Btu/h·ft^2) compared with the proposed value of 0.41 MW/m^2 (0.13 x 10^6 Btu/h·ft^2). Consequently, a preliminary evaluation of the effect of the CHF temperature oscillations at 7.2 MPa on tube fatigue life shows that it is no more severe than for the CRBRP steam generator tubes. It is of interest to note that a task force investigating strain cycling effects in the DNB zone of the CRBRP evaporators concluded

that adequate margin exists against fatigue failure.[20] Similar preliminary conclusions are drawn from a comparison of CHF temperature oscillations observed in the ANL SGTF test for simulated CRBRP 64% power conditions[21] and for conditions simulating the proposed PLBR G and P_c conditions.[22]

6. SUMMARY AND CONCLUSIONS

Characteristics of CHF and transition boiling at proposed PLBR pressures and mass flux conditions have been investigated with a tube of 10.1 mm (0.398 in.) inside diameter in a sodium-heated test facility. The investigation yielded the following principal results:

1. CHF data are presented for 7.2 MPa (1040 psia) nominal pressure and low- and high-mass flux conditions. The high-mass flux data include the nominal conditions for a proposed PLBR steam generator design, and cover the following parameter ranges:

   - mass flux 540-1490 kg/s·m^2 (0.40-1.10 10^6 lbm/h·ft^2)
   - critical heat flux 0.69-1.86 MW/m^2 (0.22-0.59 10^6 Btu/h·ft^2)
   - critical steam quality 0.48-0.89

   The low-mass flux data include conditions that might occur during inadvertently severely partially plugged tubes for a proposed PLBR steam generator design, and cover the following parameter ranges:

   - mass flux 110-270 kg/s·m^2 (0.08-0.20 10^6 lbm/h·ft^2)
   - critical heat flux 0.16-1.01 MW/m^2 (0.05-0.32 10^6 Btu/h·ft^2)
   - critical steam quality > 0.50

2. The high-mass flux data are compared to several CHF correlations available in the technical literature. A simple and more accurate correlation, Equation (4), is formulated to represent the current high-mass flux data and data obtained previously by GE with the same sodium-heated test facility. The relative standard deviation is 4.7% for all the GE data and 3.8% for the current data at 7.2 MPa. The experimental ranges of the data supporting the correlation are:

• pressure	7.0-13.0 MPa	(1015-1890 psia)
• mass flux	540-3250 kg/s•m^2	(0.40-2.40 10^6 lbm/h•ft^2)
• critical heat flux	0.69-1.86 MW/m^2	(0.22-0.59 10^6 Btu/h•ft^2)
• diameter	10.1 mm	(0.398 in.)

3. The low-mass flux data for nominal-mass flux of 260 kg/s•m^2 (0.20 x 10^6 lbm/h•ft^2) are in good agreement with the Biasi[16] correlation for high quality. For nominal mass flux of 130 kg/s ,^{2} the data show wide scatter in critical steam quality and only the data with q''_c between 0.6 and 0.9 MW/m^2 show good agreement with the Biasi[16] correlation for high quality.

4. The diameter effects on X_c predicted with several correlations are compared, and the effect predicted with the Doroschuk[11] correlation is recommended for application at proposed PLBR conditions.

5. The length of the transition boiling region experiencing temperature fluctuations is determined as 51 mm (2.0 in.) for a typical high-mass flux case and 230 mm (9.1 in.) for a typical low-mass flux case.

6. A preliminary comparison shows that the CHF temperature oscillations at conditions simulating the proposed PLBR steam generator mass flux and pressure conditions are no more severe than similar oscillations observed for simulated CRBRP 64% power conditions.

NOMENCLATURE

English Letters

C	Specific heat
D	Diameter
G	Water-side-mass flux, $kg/s \cdot m^2$
h	Heat transfer coefficient
K_{eff}	Defined when introduced
L_b	Length of nucleate boiling region
L_T	Length of the transition boiling region over which significant temperature oscillations occur
P_c	Pressure at CHF
$P_{c,r}$	Reduced pressure at CHF, $P_c/22.12$ for P_c in MPa ($P_c/3208.2$ for P_c in psia)
q"	Heat flux based on i.d. of tube
$\bar{q}''_b$	Average heat flux over the nucleate boiling length
T	Temperature
T_s	Average shell temperature at each station
W	Mass flow rate
X	Mass quality
Z	Axial location along tube from water inlet

Greek Letters

β	Spacer adjustment factor
σ	Relative standard deviation

Subscripts

c	Refers to conditions at the CHF location
cor	Correlation
exp	Experiment
i	Tube inside surface
N	Sodium side
o	Tube outside surface
s	Shell outside surface
$X_{10.1}$	Refers to critical steam quality at D_i = 10.1 mm
$X_{31.3}$	Refers to critical steam quality at D_i = 31.3 mm

REFERENCES

1. J. Y. Hwang, L. E. Efferding, and R. P. Waszink, "Sodium-Heated Evaporator Critical Heat Flux Experiments at Subcritical Pressure Conditions for Commercial LMFBR Plant Application," ASME Paper No. 76-JPGC-NE-10, September 1976.

2. S. Wolf and D. H. Holmes, "Critical Heat Flux in a Sodium-Heated Steam Generator Tube," General Electric Co., FBRD, GEFR-SP001, January 1977.

3. S. Wolf and D. H. Holmes, "Thermal/Hydraulic Test Results Including Critical Heat Flux Conditions for a Sodium-Heated Steam Generator Tube Model," General Electric Co., FBRD, NEDM-14150, September 1976.

4. D. J. Rush and P. B. Stephens, Responsible Engineers, "DNB Effects Test Section," General Electric Co., FBRD, Doc. No. 22A3554, Rev. 5, September 15, 1975.

5. E. D. Sweeney, Responsible Engineer, "DNB Effects Test Loop," General Electric Co., FBRD, Doc. No. 22A3960, Rev. 3, February 1976.

6. S. Wolf, "Instrument Specification and Test Matrix for PLBR Testing in the DNB Loop," General Electric Co., FBRD, FBRD-00002(L), January 5, 1977.

7. O. E. Dwyer, "On the Transfer of Heat to Fluids Flowing Through Pipes, Annuli, and Parallel Plates," Nuclear Science and Engineering, Vol. 17, 1963, pp. 336-344.

8. O. E. Dwyer and P. S. Tu, "Unilateral Heat Transfer to Liquid Metals Flowing in Annuli," Nuclear Science and Engineering, Vol. 15, 1962, pp. 58-68.

9. J. G. Collier, Convective Boiling and Condensation, McGraw-Hill Book Company, London, 1972, pp. 129-135.

10. L. E. Efferding, J. Y. Hwang, and R. P. Waszink, "Experimental Evaluation of Critical Heat Flux in Film Boiling Behavior in a Sodium-Heated Duplex Tube Steam Generator Model," AIChE Paper No. 99C, AIChE Annual Meeting, November 1975.

11. V. E. Doroschuk, L. L. Levitan, and F. P. Lantzman, "Investigations Into Burnout in Uniformly Heated Tubes," ASME Paper No. 75-WA/HT-22, November 1975.

12. D. M. France, T. Chiang, and R. D. Carlson, "Early Results for CRBR 100% and 64% Loads," Argonne National Laboratory, CT/HT0754, July 8, 1976.

13. S. Bertoletti, et al., "Heat Transfer Crisis in Steam-Water Mixtures," Energie Nucleare, Vol. 12, No. 3, 1965, pp. 121-172.

14. D. M. France, T. Chiang, R. D. Carlson, and T. Tsuchiya, "Initial CHF Data From SGTF Experiments," Argonne National Laboratory, CT/HT0949, January 12, 1977.

15. D. M. France, T. Chiang, and R. D. Carlson, "CHF Data at 7.00 MPa and 7.34 MPa," Argonne National Laboratory, CT/HT1016, March 3, 1977.

16. L. Biasi, et al., "Studies on Burnout: Part 3, A New Correlation for Round Ducts and Uniform Flux and Its Comparison With World Data," Energie Nucleare, Vol. 14, No. 9, 1967, pp. 530-536.

17. A. S. Kon'kov, "Experimental Study of the Conditions Under Which Heat Exchange Deteriorates When a Steam-Water Mixture Flows in Heated Tubes," Thermal Engineering, translated from Teploenergetika, Vol. 13, No. 12, 1966, pp. 53-57.

18. G. J. Kirby, "A New Correlation of Non-uniformly Heated Round Tube Burnout Data," AEEW-R500, 1966.

19. B. Thompson and R. V. Macbeth, "Boiling Water Heat Transfer Burnout in Uniformly Heated Round Tubes: A Compilation of World Data With Accurate Correlations," AEEW-R356, 1964.

20. P. M. Magee, D. F. Casey, C. L. Chu, C. W. Dillmann, J. M. Roberts, and S. Wolf, "An Evaluation of Strain Cycling Effects in the DNB Zone of the CRBR Evaporators," General Electric Co., FBRD, NEDM-14164, December 1976.

21. D. M. France, T. Chiang, and R. D. Carlson, "Additional Low Flow Tests in the SGTR," Argonne National Labortory, CT/HT0832, October 11, 1976.

22. D. M. France, "Temperature Recordings for ANL-SGTF Tests R326, R333," Argonne National Laboratory, CT/HT1025, March 15, 1977.

APPENDIX A

SUMMARY OF CHF DATA

This appendix* consists of Tables A-1 and A-2, summarizing the CHF data generated during the current investigation at 7.2 MPa nominal pressure.

*Conversion factors:

(MPa) = (psia)/145.04

$(kg/s \cdot m^2) = (lbm/h \cdot ft^2)/737.4$

$(W/m^2) = 3.1525\ (Btu/h \cdot ft^2)$

(m) = 0.3048 (ft)

Table A-1
CHF RESULTS FOR HIGH MASS FLUX AT 7.2 MPa

Run No.	Test No.	P_c (psia)	G 10^6 lbm/ h·ft^2	q''_c 10^6 Btu/ h·ft^2	$\bar{q}''_b$ 10^6 Btu/ h·ft^2	L_b (ft)	X_c
1	20.1	1039.	1.056	0.539	0.196	13.60	0.502
2	20.1	1025.	1.071	0.518	0.199	13.70	0.502
3	20.1	1032.	1.080	0.478	0.204	13.70	0.506
4	20.2	1037.	1.068	0.524	0.193	14.10	0.479
5	20.2	1032.	1.069	0.512	0.202	13.60	0.484
6	20.2	1060.	1.067	0.430	0.199	13.90	0.492
7	20.2	1046.	1.075	0.469	0.201	13.70	0.482
8	20.2	1028.	1.066	0.574	0.216	13.10	0.498
9	21.1	1048.	1.101	0.418	0.197	14.70	0.511
10	21.2	1047.	1.096	0.332	0.202	14.40	0.504
11	22.1	1037.	0.993	0.526	0.194	13.70	0.531
12	22.1	1046.	0.995	0.478	0.190	14.10	0.532
13	22.2	1033.	0.986	0.489	0.197	13.80	0.517
14	22.2	1045.	1.008	0.442	0.199	13.80	0.513
15	22.3	1035.	0.984	0.536	0.214	13.00	0.531
16	22.3	1054.	1.007	0.589	0.219	12.70	0.524
17	23.1	1041.	0.996	0.386	0.188	15.10	0.552
18	23.2	1046.	0.988	0.299	0.198	14.40	0.547
19	23.3	1054.	0.978	0.353	0.218	12.70	0.535
20	24.1	1043.	0.800	0.557	0.179	13.80	0.608
21	24.2	1019.	0.804	0.441	0.181	14.10	0.593
22	24.2	1016.	0.805	0.450	0.182	14.10	0.593
23	24.3	1047.	0.803	0.518	0.193	13.10	0.595
24	24.4	1029.	0.809	0.538	0.209	12.20	0.591
25	24.5	1020.	0.810	0.404	0.222	11.20	0.575
26	25.1	1040.	0.805	0.455	0.180	14.50	0.632
27	25.2	1047.	0.801	0.374	0.185	14.00	0.610
28	25.3	1043.	0.800	0.333	0.195	13.00	0.598
29	25.4	1046.	0.808	0.352	0.207	12.40	0.598
30	25.5	1044.	0.803	0.314	0.215	12.00	0.603
31	26.1	1042.	0.600	0.445	0.142	15.10	0.700
32	26.2	1055.	0.593	0.411	0.161	13.80	0.707
33	26.3	1024.	0.591	0.465	0.169	13.00	0.699
34	26.5	1064.	0.590	0.364	0.197	10.90	0.689
35	26.7	1045.	0.597	0.414	0.256	8.80	0.712
36	27.1	1040.	0.603	0.315	0.158	14.80	0.738
37	27.2	1062.	0.533	0.373	0.155	14.20	0.718
38	27.3	1058.	0.606	0.265	0.171	13.30	0.707
39	27.5	1064.	0.604	0.304	0.183	12.20	0.703
40	27.6	1055.	0.598	0.319	0.202	10.80	0.689
41	27.7	1069.	0.592	0.374	0.219	9.80	0.686
42	28.1	1049.	0.406	0.384	0.137	13.20	0.876
43	28.2	1054.	0.402	0.308	0.140	12.80	0.841
44	28.3	1043.	0.407	0.374	0.147	12.10	0.823
45	28.4	1044.	0.403	0.371	0.149	12.50	0.864
46	28.5	1047.	0.404	0.286	0.155	11.30	0.817
47	28.6	1052.	0.435	0.424	0.160	11.90	0.823
48	29.1	1043.	0.410	0.354	0.128	14.40	0.883
49	29.2	1028.	0.409	0.221	0.131	14.50	0.870
50	29.3	1043.	0.410	0.253	0.141	12.70	0.820
51	29.4	1033.	0.414	0.252	0.135	14.50	0.889
52	29.5	1053.	0.411	0.252	0.157	12.20	0.881
53	29.6	1042.	0.407	0.241	0.173	11.20	0.894

Table A-2
CHF RESULTS FOR LOW MASS FLUX AT 7.2 MPa

Run No.	Test No.	P_c (psia)	G 10^6 lbm/ h·ft^2	q''_c 10^6 Btu/ h·ft^2	$\bar{q}''_b$ 10^6 Btu/ h·ft^2	L_b (ft)	X_c
1	30.1	1077.	0.197	0.163	0.074	13.70	0.997
2	30.1	1048.	0.195	0.117	0.057	14.80	0.845
3	30.2	1043.	0.191	0.157	0.062	13.30	0.802
4	30.2	1037.	0.204	0.166	0.063	14.00	0.907
5	30.3	1063.	0.190	0.170	0.073	11.00	0.795
6	30.4	1057.	0.193	0.143	0.078	10.50	0.803
7	30.5	1041.	0.193	0.144	0.084	9.90	0.802
8	30.6	1070.	0.193	0.145	0.084	9.60	0.794
9	30.7	1067.	0.195	0.160	0.090	8.70	0.766
10	31.1	1040.	0.197	0.094	0.059	15.10	0.863
11	31.2	1055.	0.197	0.084	0.062	14.60	0.864
12	31.3	1056.	0.197	0.141	0.075	12.00	0.865
13	31.4	1045.	0.196	0.122	0.071	12.30	0.842
14	31.5	1041.	0.196	0.143	0.087	10.40	0.869
15	31.6	1059.	0.195	0.144	0.096	9.30	0.863
16	34.1	1043.	0.195	0.319	0.089	8.80	0.835
17	34.2	1048.	0.195	0.238	0.088	8.90	0.755
18	34.3	1054.	0.196	0.317	0.096	10.10	0.933
19	34.4	1052.	0.194	0.276	0.112	8.00	0.870
20	32.1	1052.	0.104	0.079	0.026	12.80	0.639
21	32.2	1055.	0.094	0.058	0.026	12.50	0.652
22	32.3	1033.	0.089	0.054	0.029	12.10	0.738
23	32.7	1049.	0.093	0.081	0.043	9.70	0.801
24	35.1	1047.	0.098	0.127	0.043	5.50	0.527
25	35.2	1047.	0.101	0.125	0.047	5.70	0.495
26	35.3	1046.	0.087	0.134	0.061	6.20	0.819
27	35.4	1061.	0.081	0.153	0.062	5.60	0.809
28	36.1	1036.	0.098	0.266	0.069	6.00	0.946
29	36.2	1040.	0.097	0.223	0.071	5.80	0.793
30	36.3	1044.	0.099	0.208	0.067	7.30	0.918
31	36.4	1051.	0.099	0.290	0.094	5.90	1.000
32	36.5	1052.	0.097	0.210	0.083	6.10	0.979

APPENDIX B

TEMPERATURE AND HEAT FLUX DISTRIBUTIONS WITH CHF

This appendix* consists of Figures B-1 through B-16 showing typical temperature and heat flux distributions for each test series.

*Conversion factors:

(MPa) = (psia)/145.04

($kg/s \cdot m^2$) = ($lbm/h \cdot ft^2$)/737.4

(W/m^2) = 3.1525 ($Btu/h \cdot ft^2$)

(m) = 0.3048 (ft)

(kg/s) = (lbm/h)/7936.5

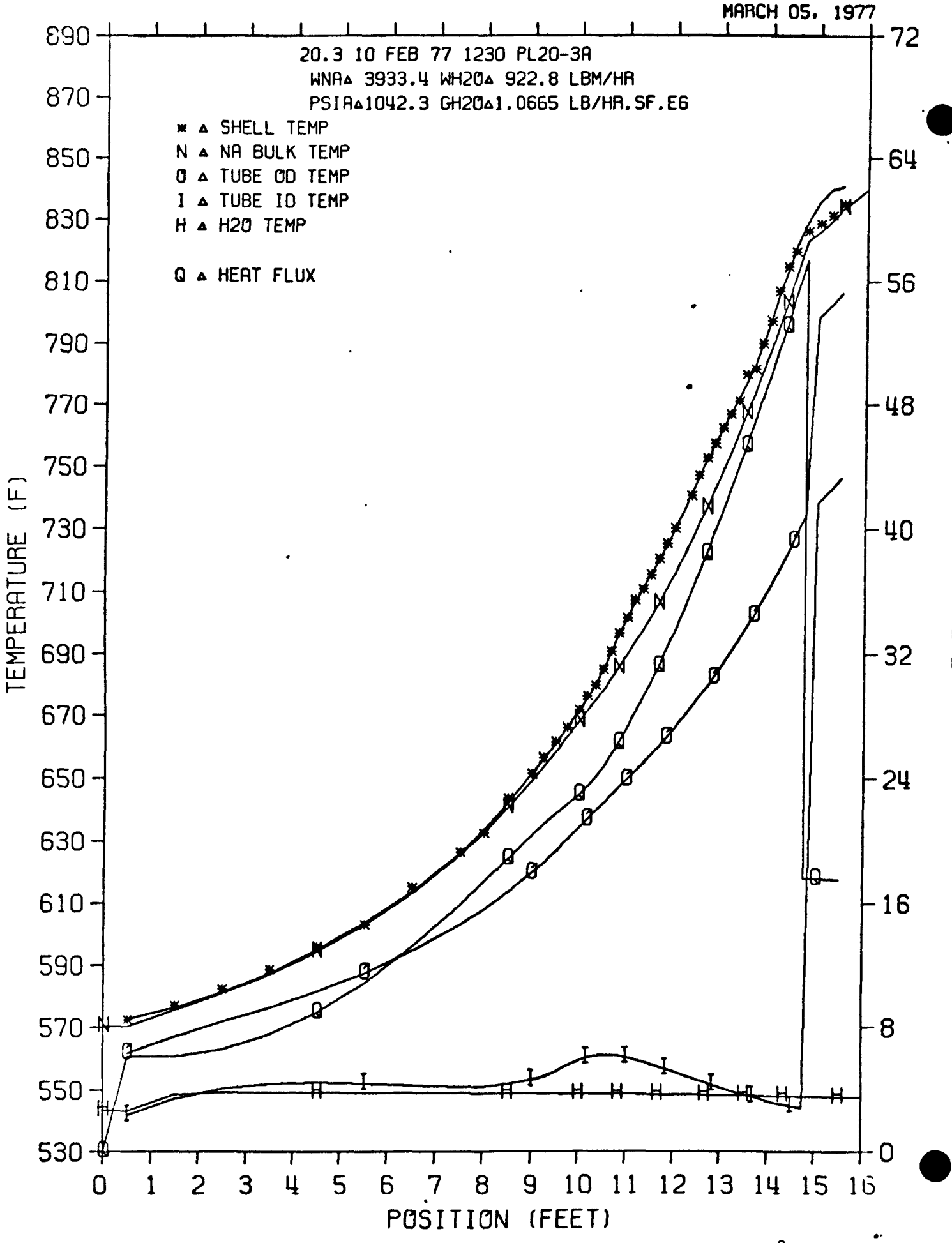

Figure B-1. Heat Flux and Temperature Distribution, Test 20.3, G = 1440 kg/s. m^2

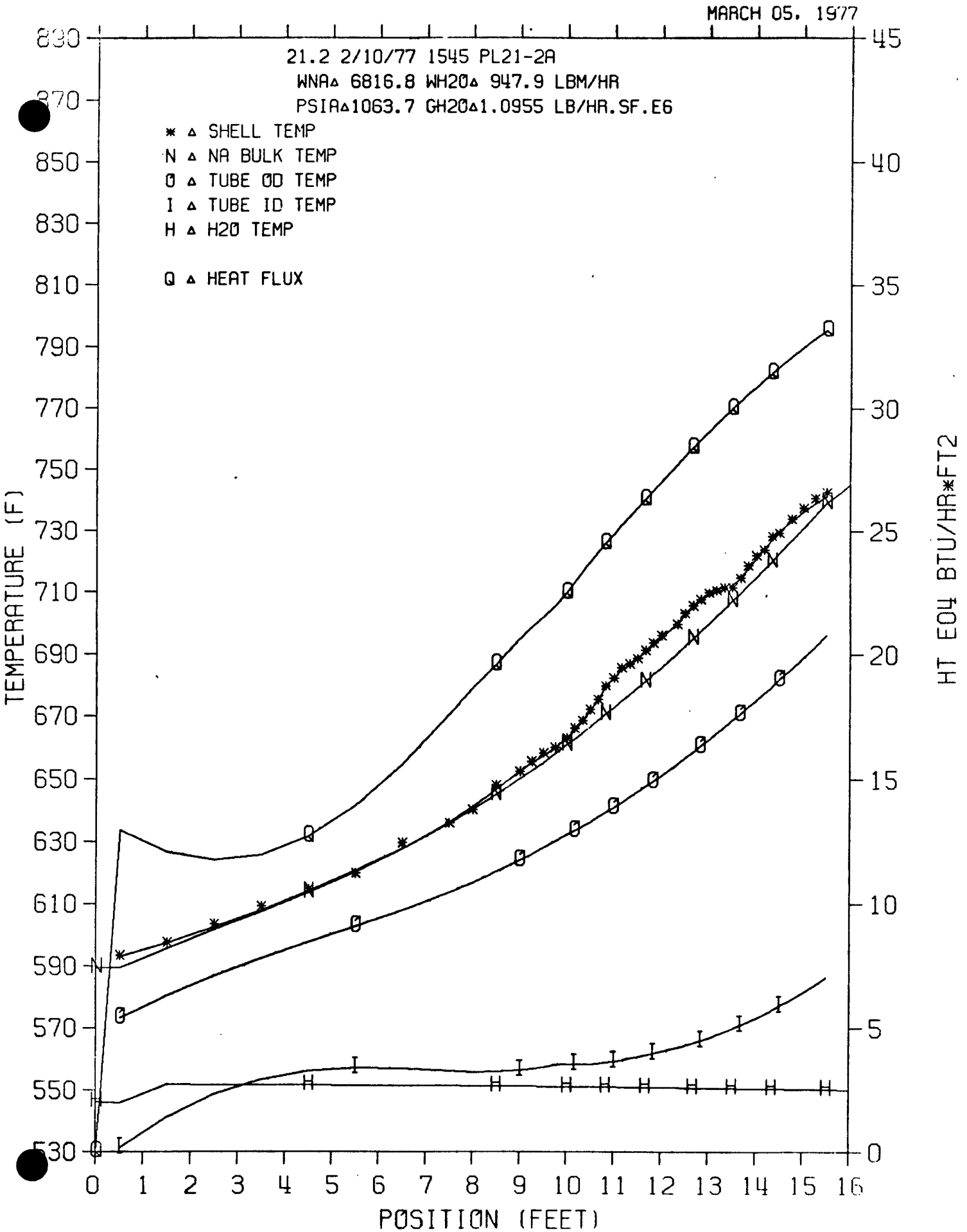

Figure B-2. Heat Flux and Temperature Distribution, Test 21.2, G = 1485 kg/s · m²

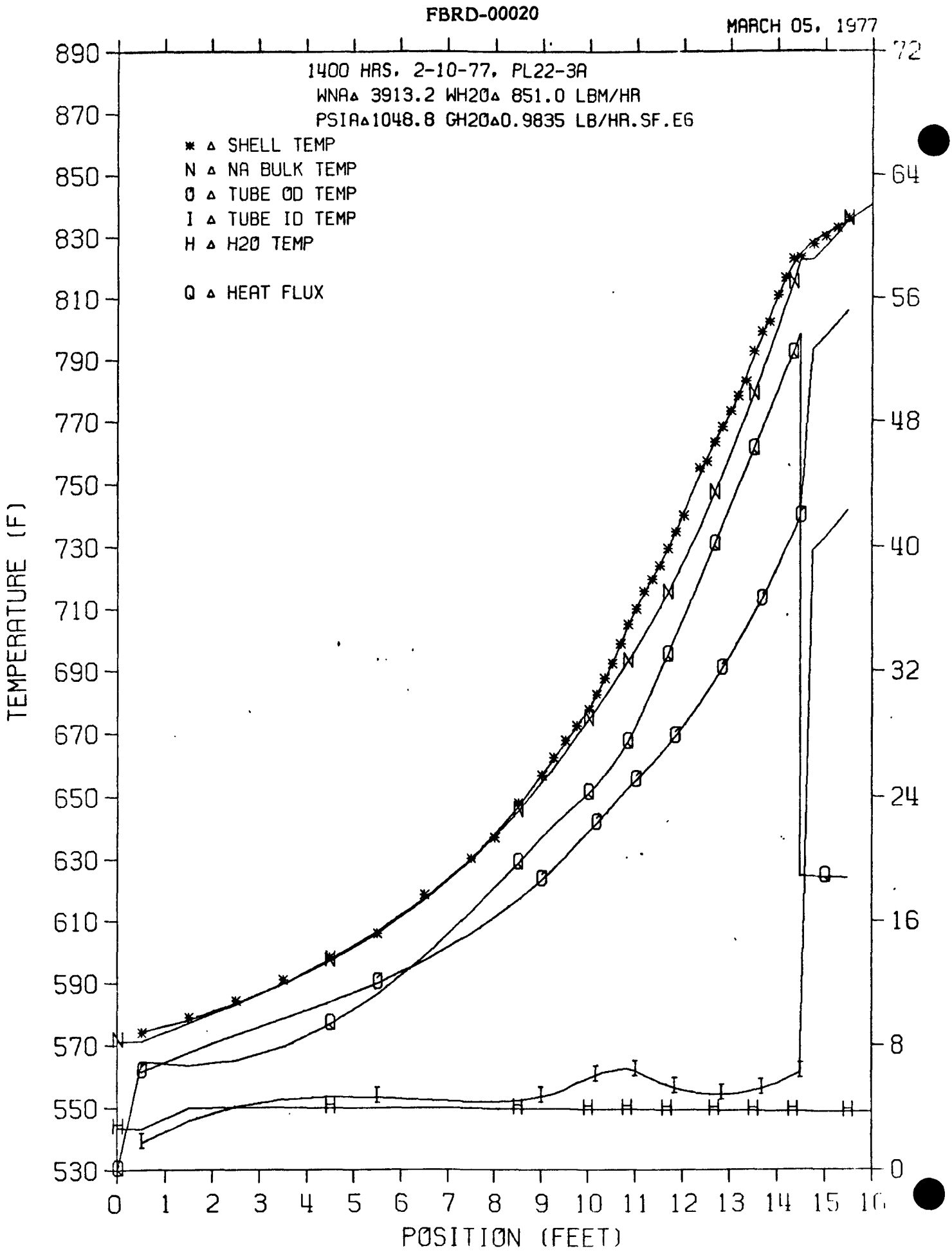

Figure B-3. Heat Flux and Temperature Distribution, Test 22.3, G = 1334 kg/s. m^2

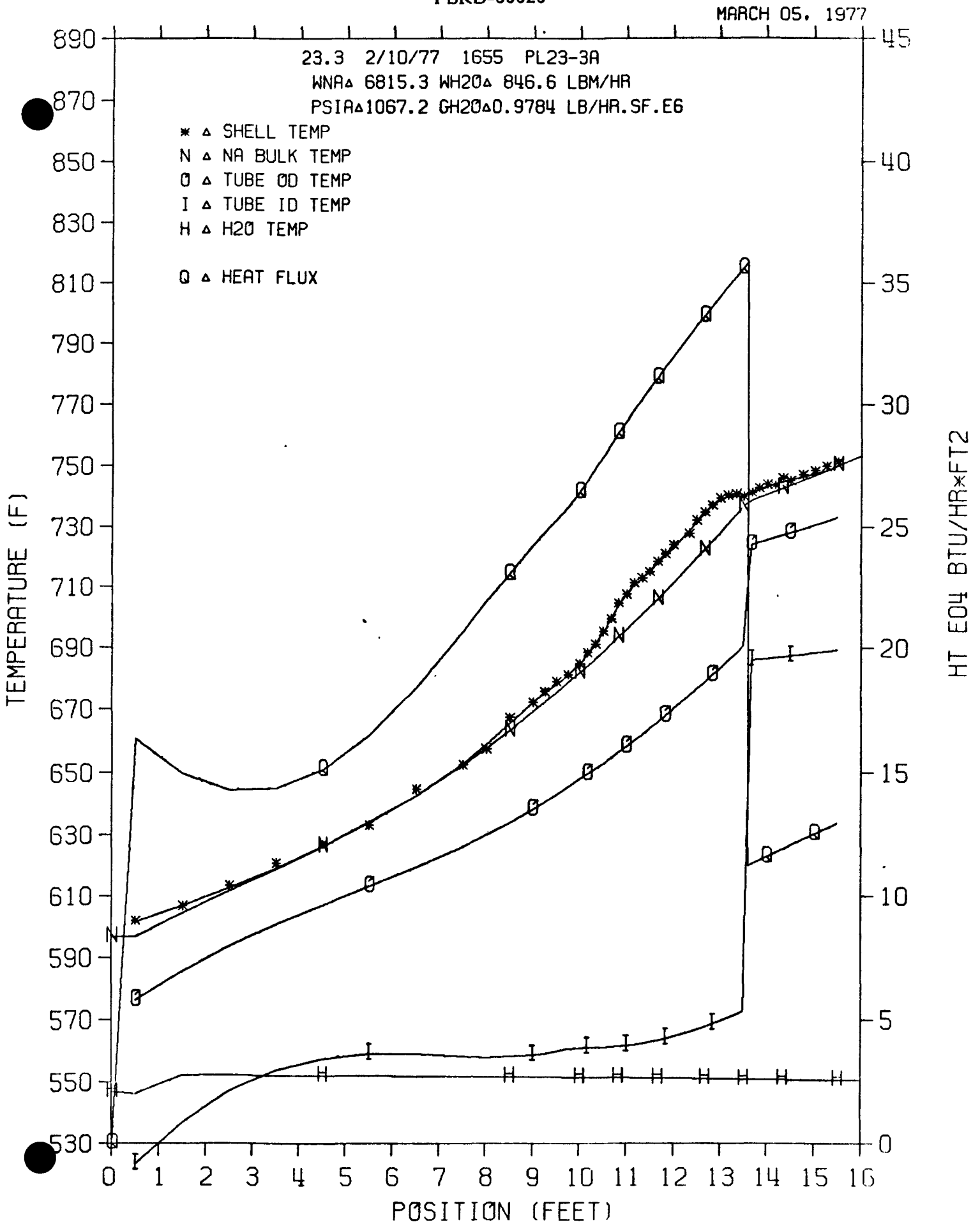

Figure B-4. Heat Flux and Temperature Distribution, Test 23.3, G = 1327 kg/s. m^2

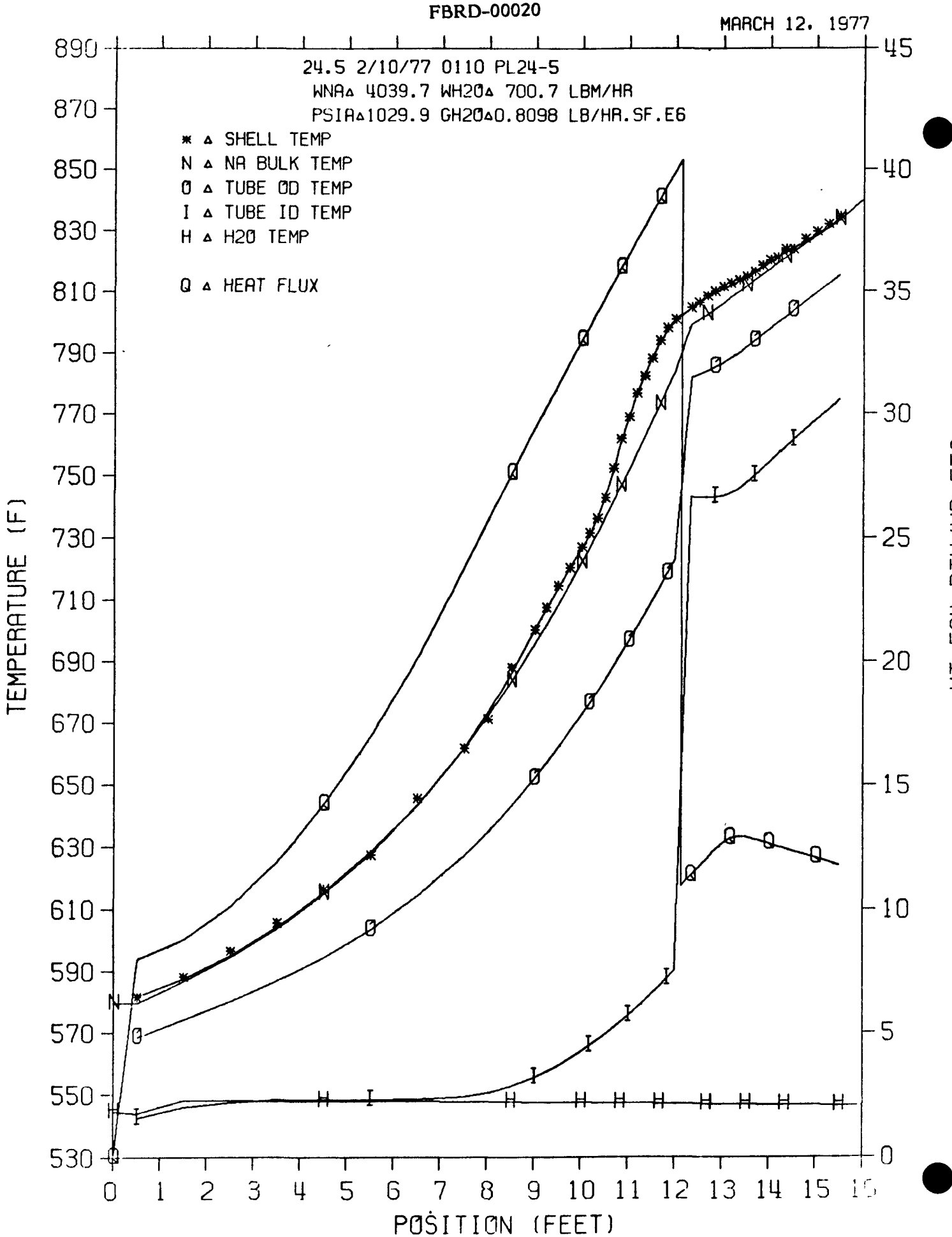

Figure B-5. Heat Flux and Temperature Distribution, Test 24.5, G = 1098 kg/s.m^2

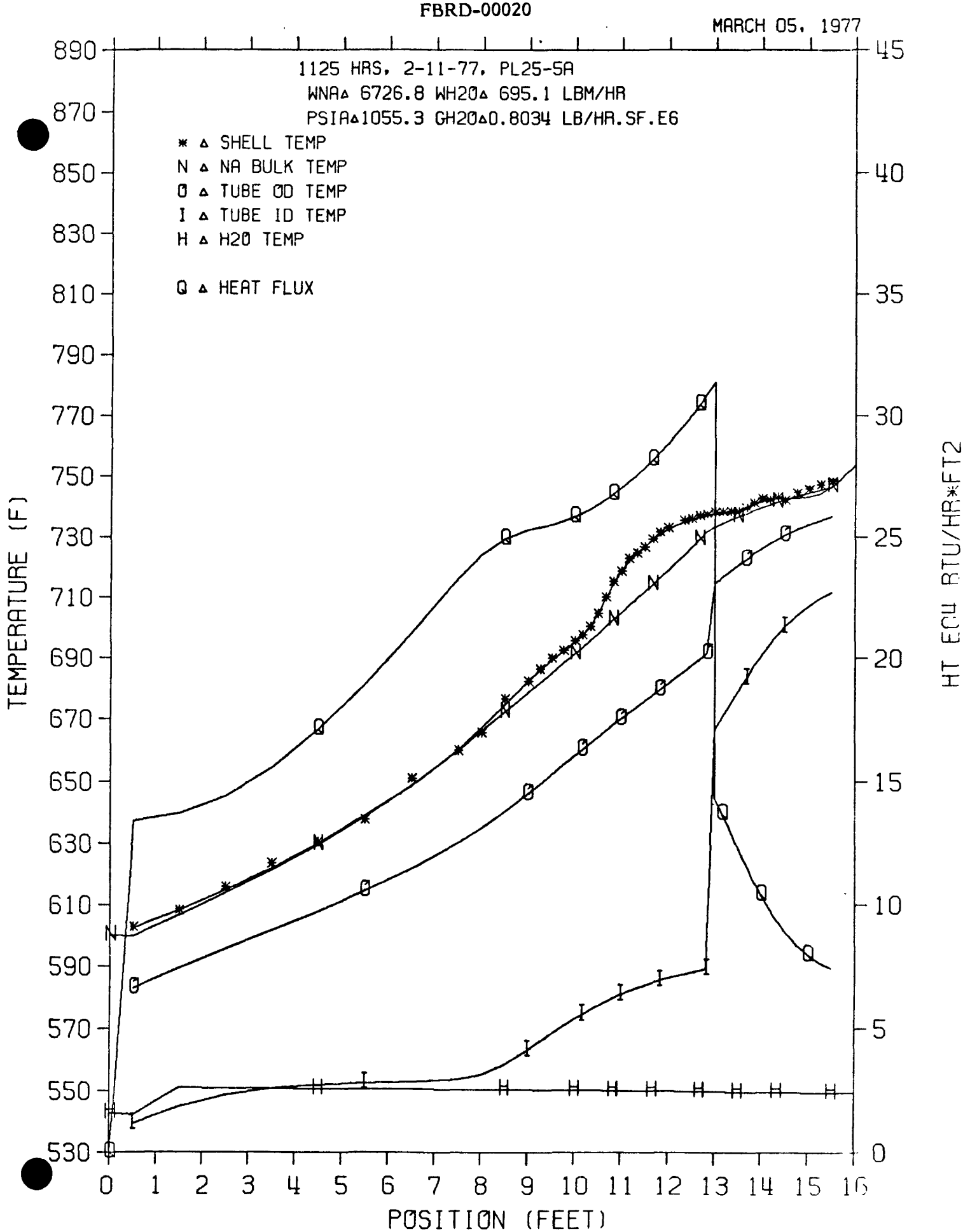

Figure B-6. Heat Flux and Temperature Distribution, Test 25.5, G = 1089 kg/s . m²

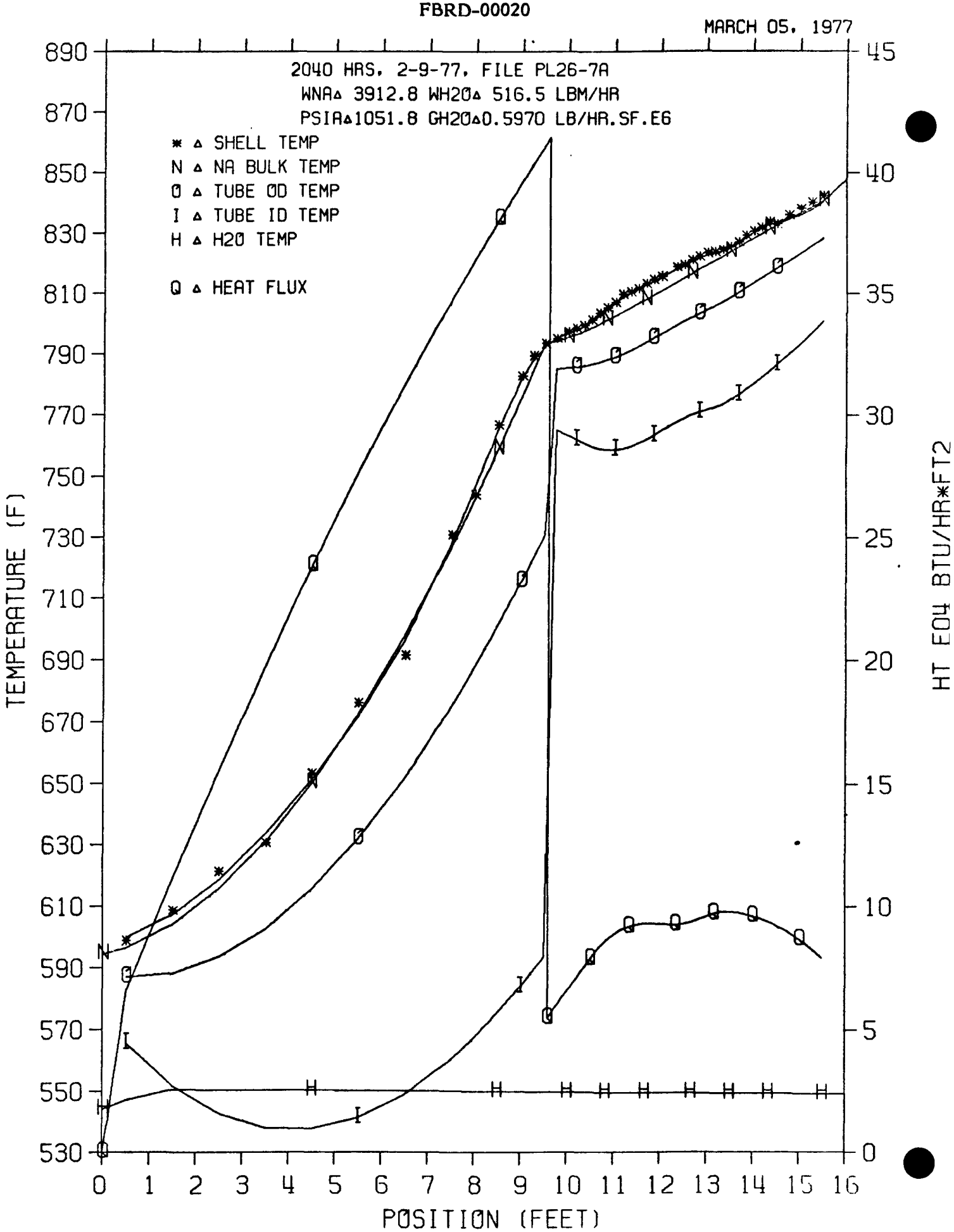

Figure B-7. Heat Flux and Temperature Distribution, Test 26.7, G = 810 kg/s. m^2

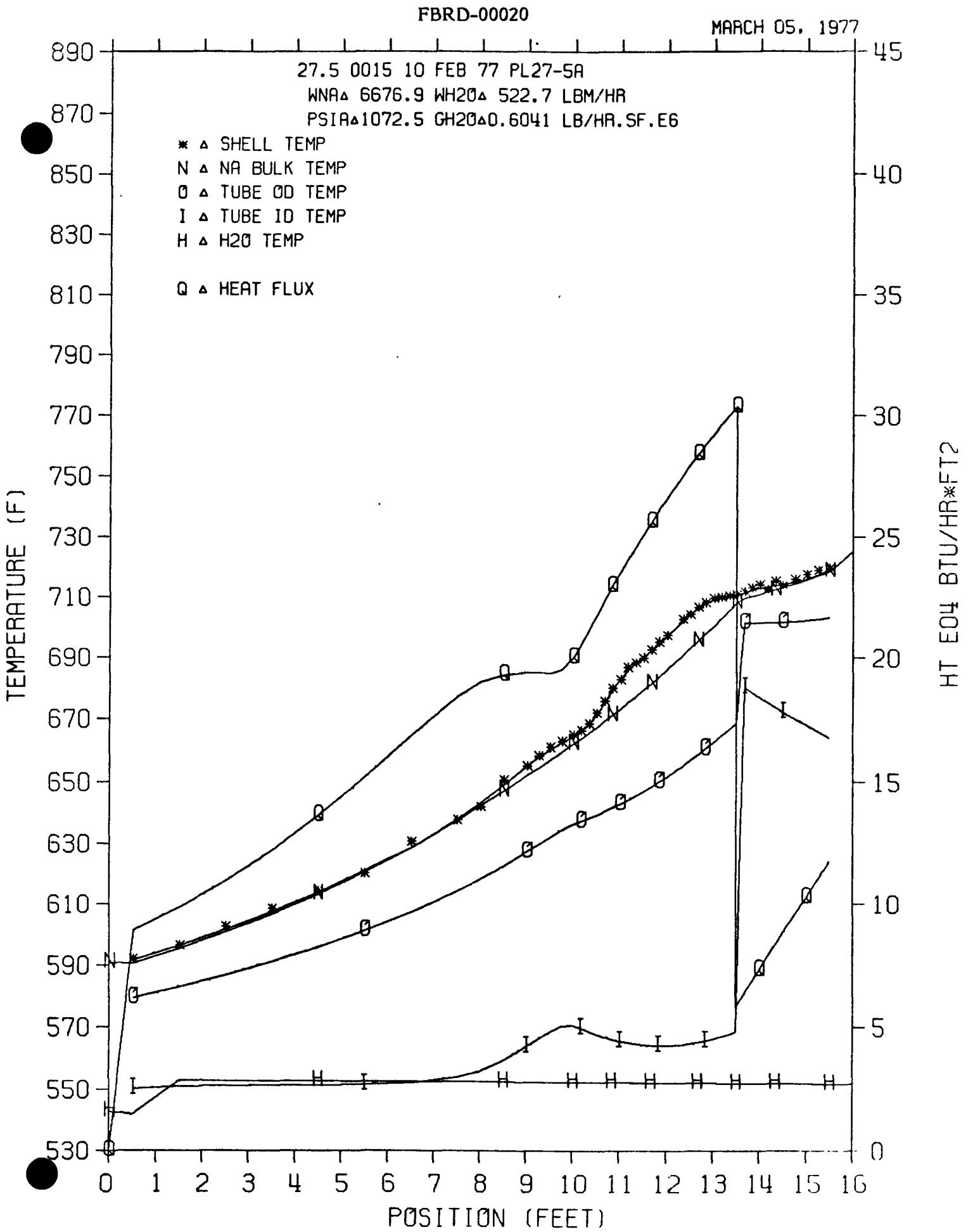

Figure B-8. Heat Flux and Temperature Distribution, Test 27.5, G = 819 kg/s . m^2

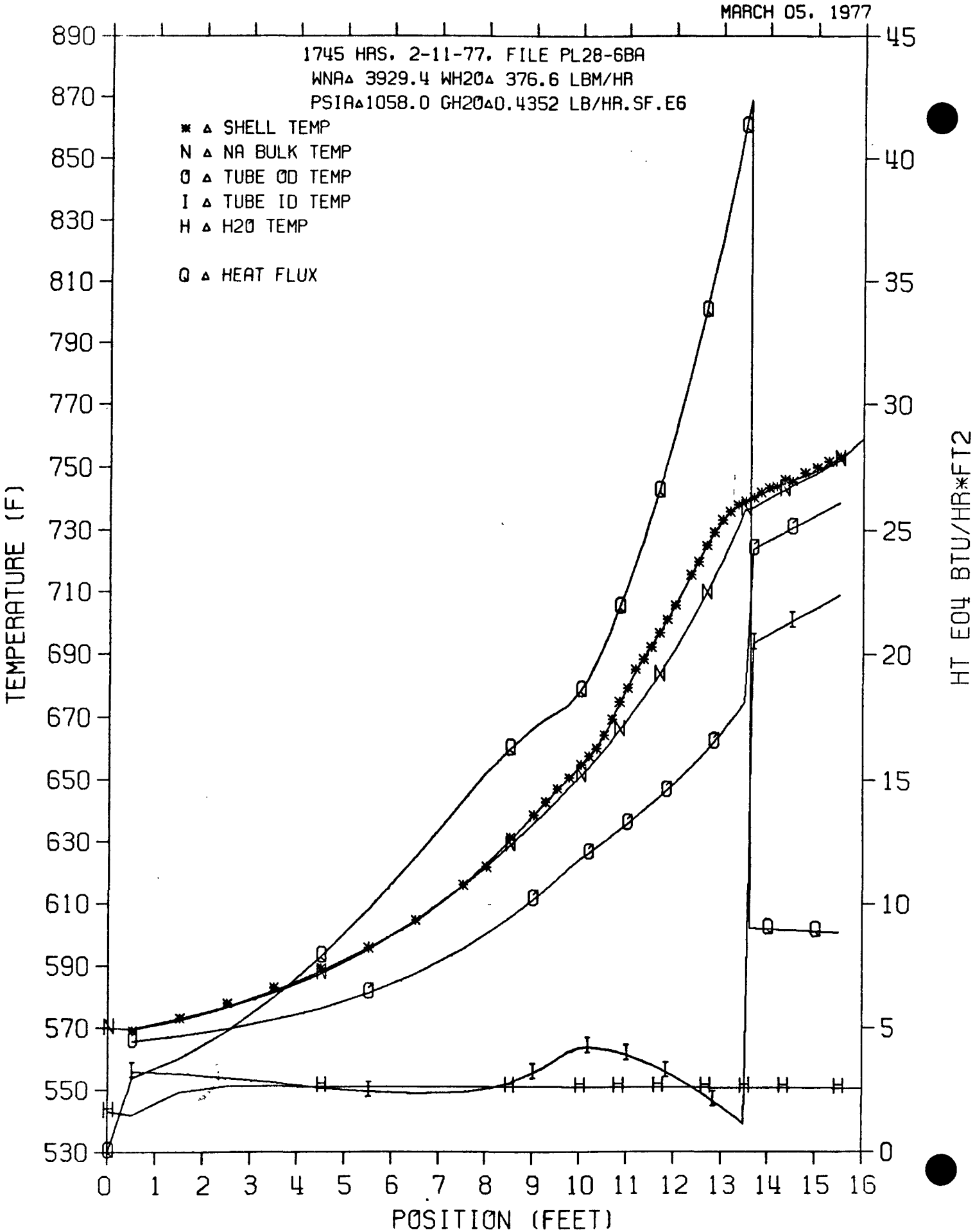

Figure B-9. Heat Flux and Temperature Distribution, Test 28.6, G = 590 kg/s · m²

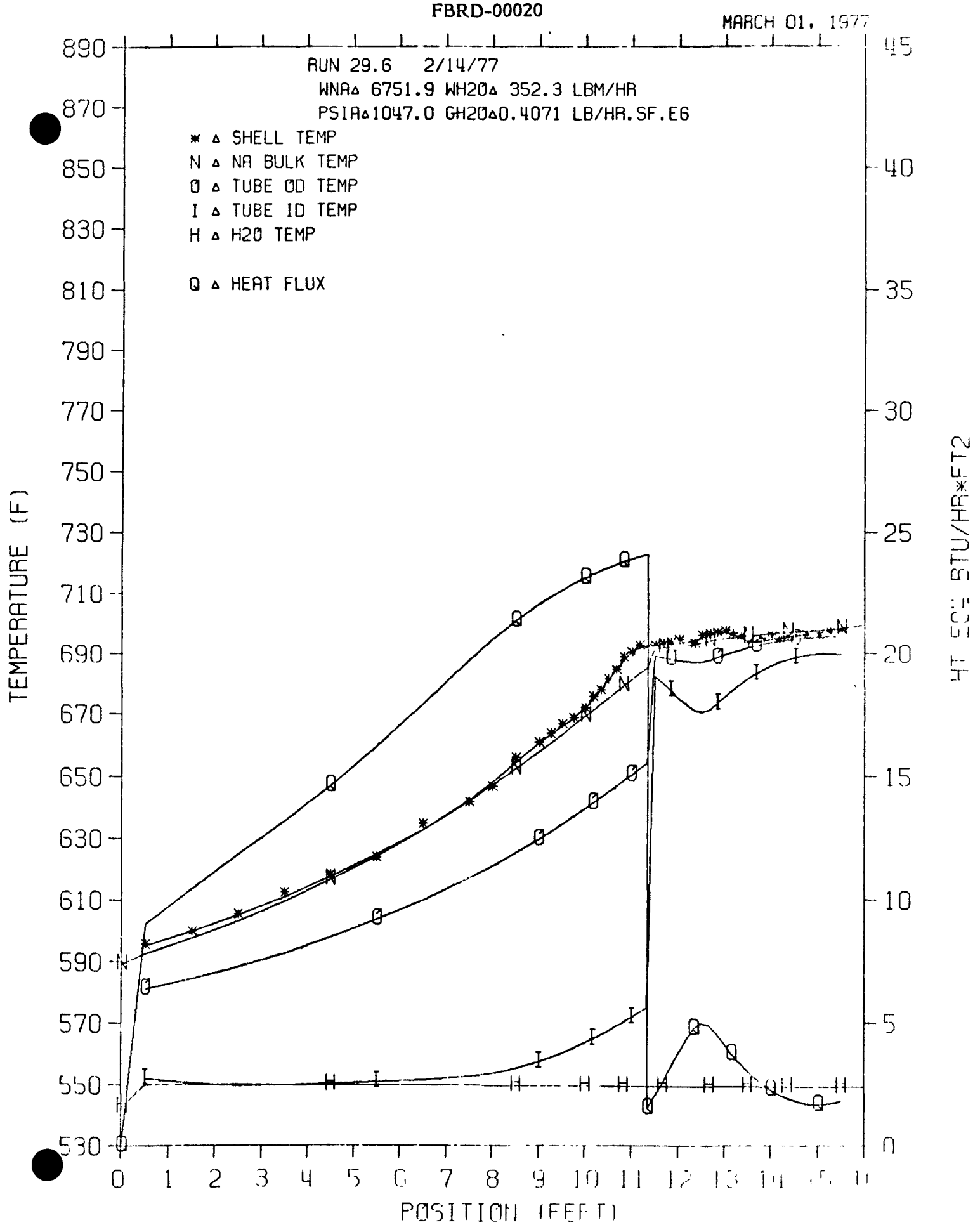

Figure B-10. Heat Flux and Temperature Distribution, Test 29.6, G = 552 kg/s . m^2

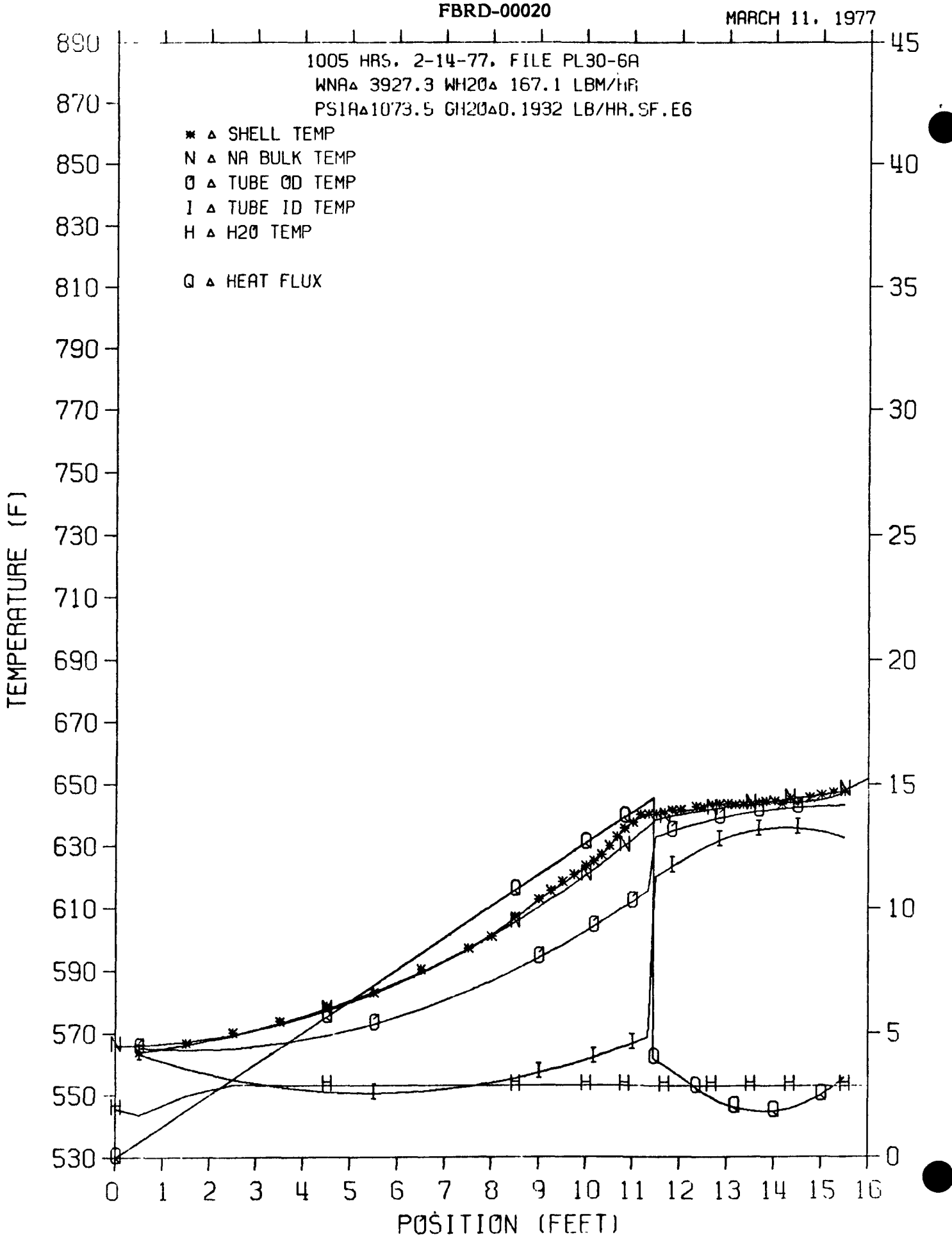

Figure B-11. Heat Flux and Temperature Distribution, Test 30.6, G = 262 kg/s . m²

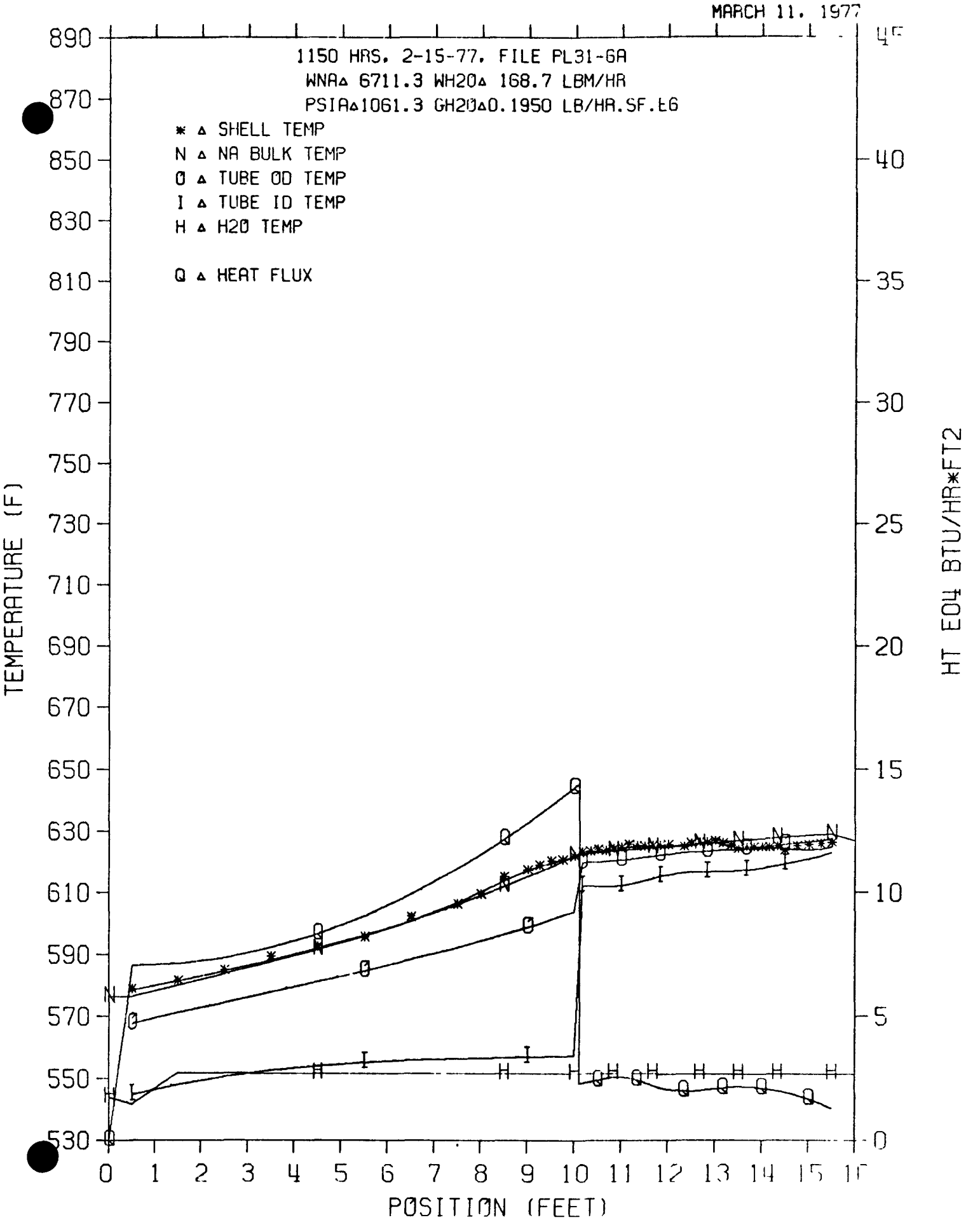

Figure B-12. Heat Flux and Temperature Distribution, Test 31.6, G = 264 kg/s . m^2

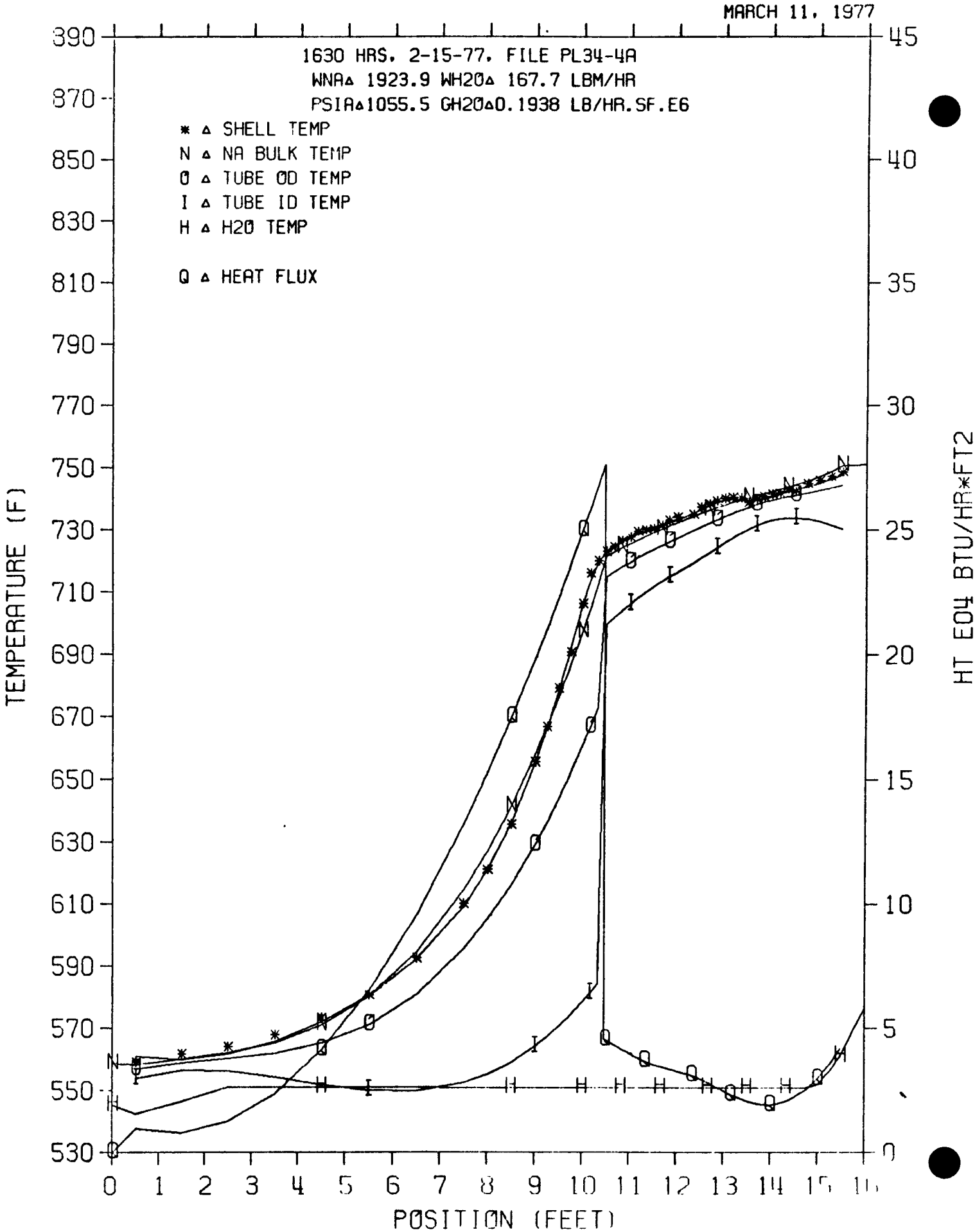

Figure B-13. Heat Flux and Temperature Distribution, Test 34.4, G = 263 kg/s . m²

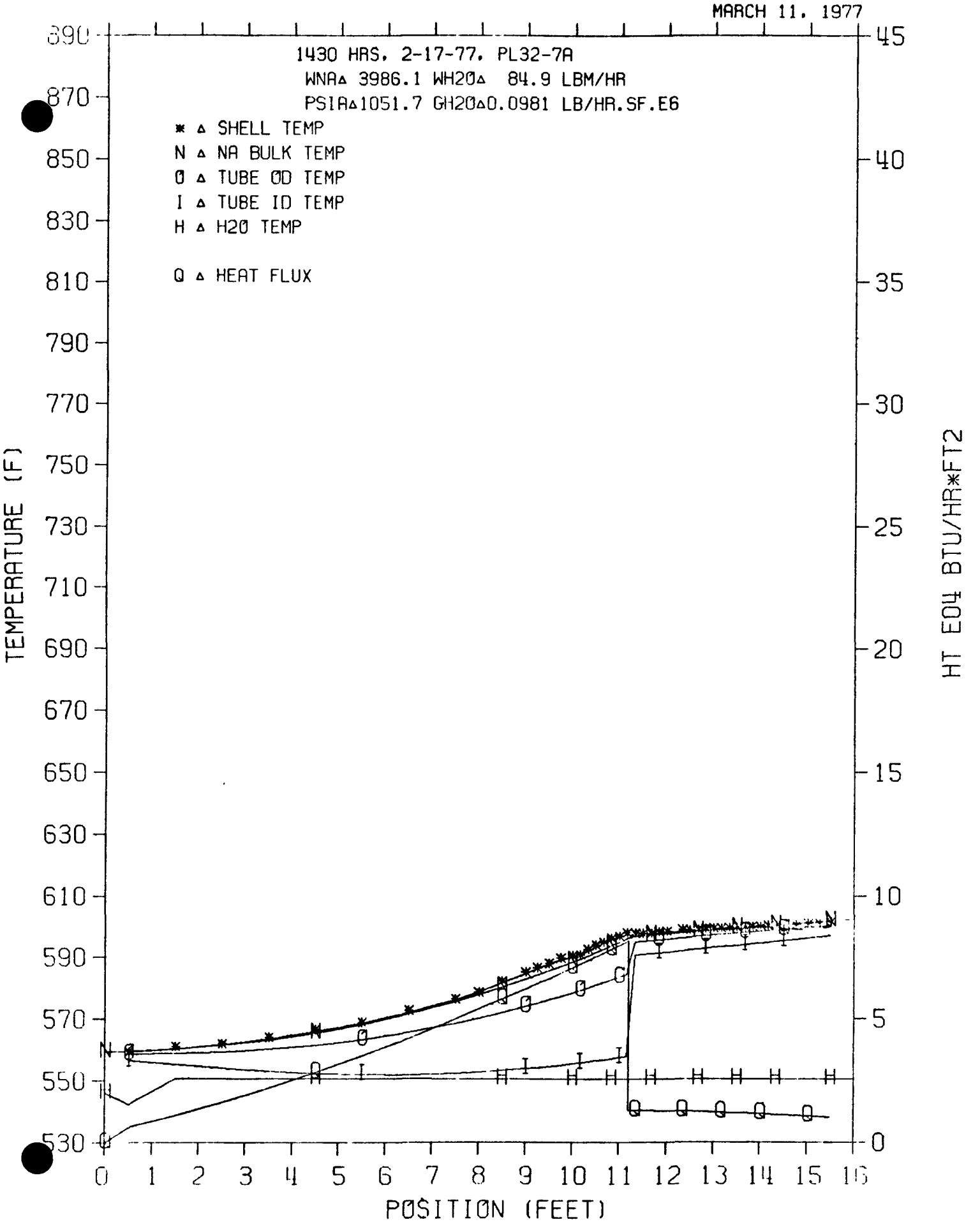

Figure B-14. Heat Flux and Temperature Distribution, Test 32.7, G = 133 kg/s . m²

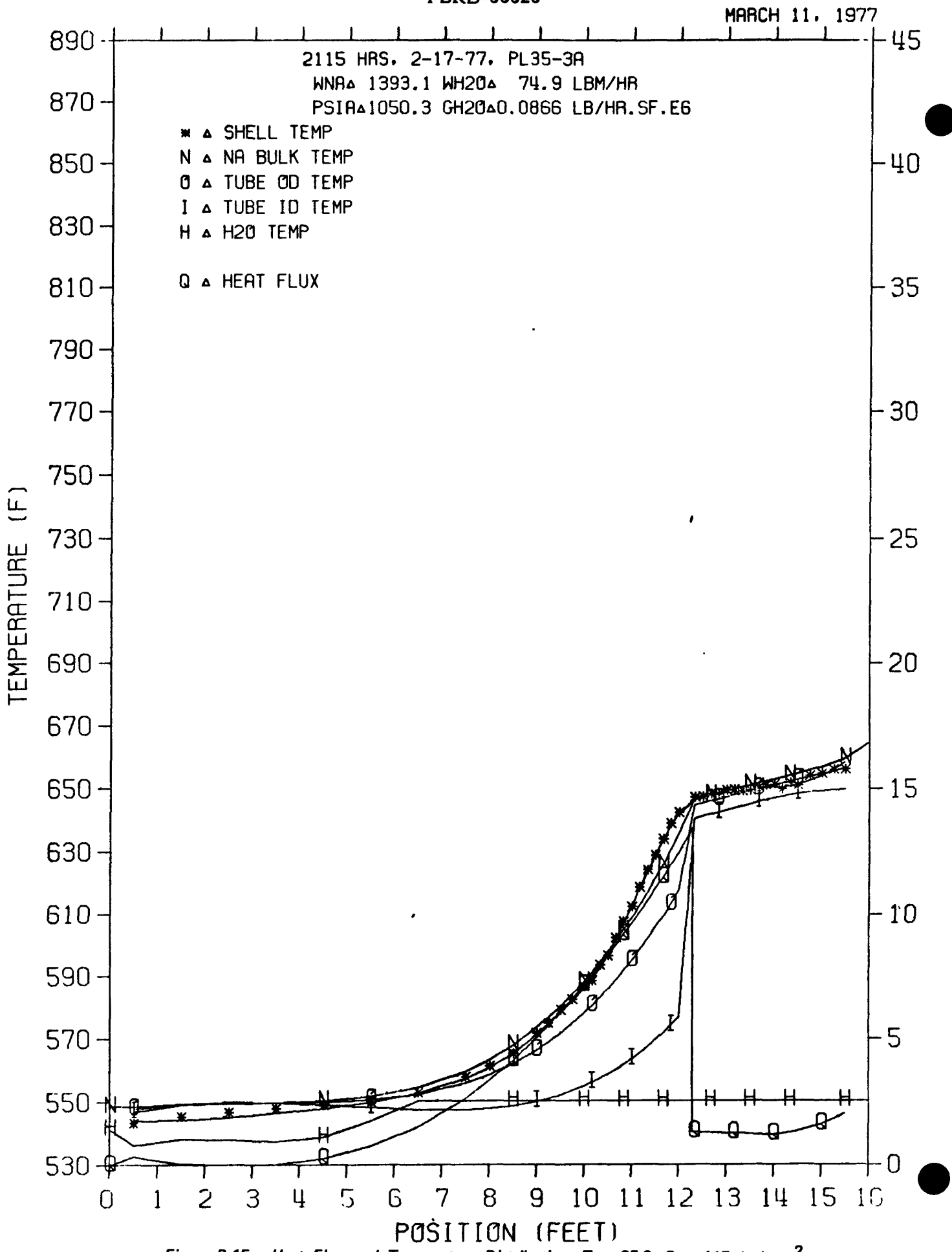

Figure B-15. Heat Flux and Temperature Distribution, Test 35.3, G = 117 kg/s.m²

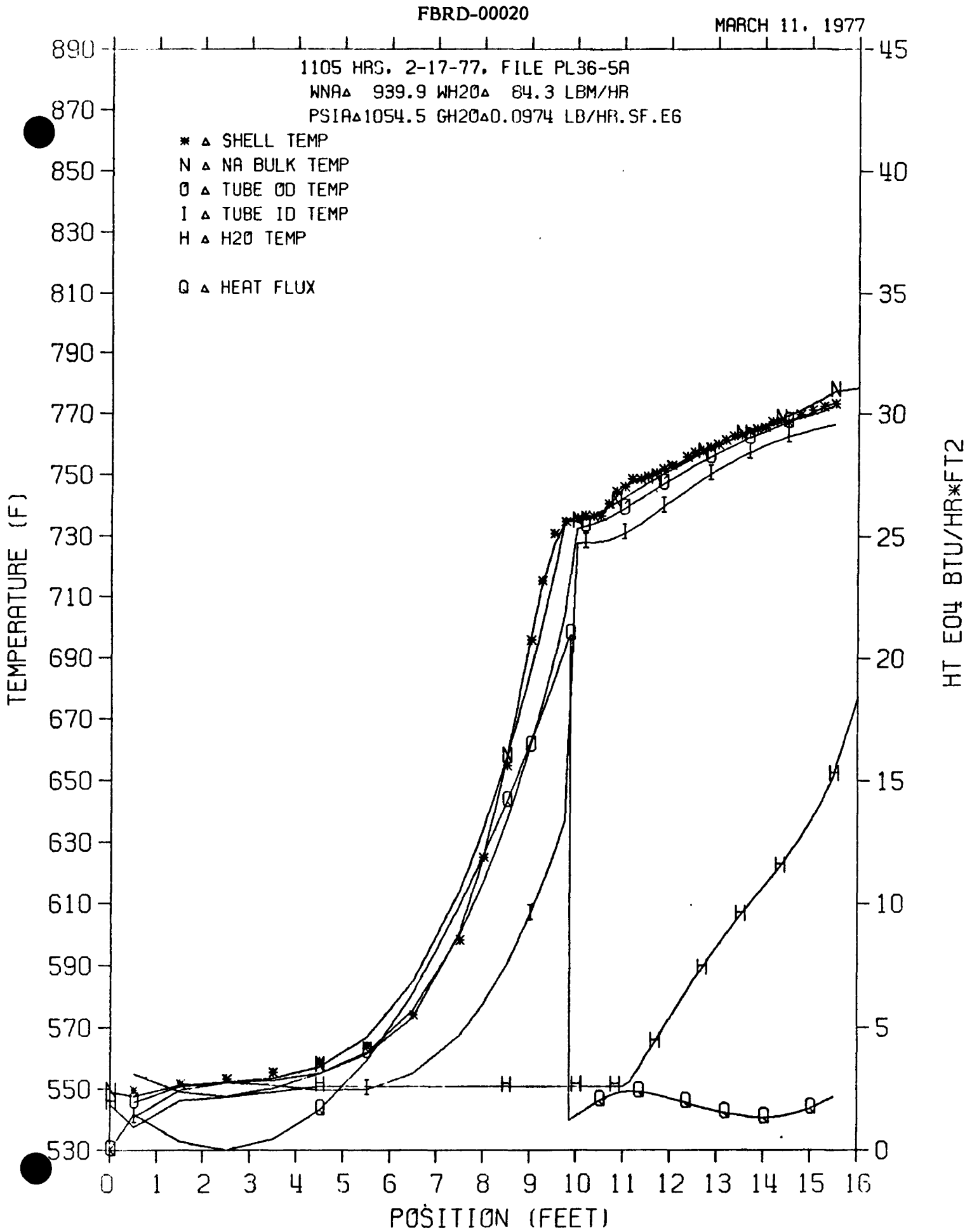

Figure B-16. Heat Flux and Temperature Distribution, Test 36.5, G = 132 kg/s.m²

DISTRIBUTION

		No. of Copies
ERDA-WDC		
W. R. Kornack, Project Group, PLBR Design Projects		3
J. Ford, Chief, Component Development		1
J. Hopenfeld		1
EPRI - Palo Alto		
J. G. Duffy, ERDA-EPRI LMFBR Design Projects		6
ANL		
W. R. Simmons		1
D. M. France		1
Bechtel - San Francisco		
S. Golan, LMFBR Design Projects		4
FWEC		
B. E. Dawson, Project Manager		3
W-Tampa		
R. Waszink		1
GE-FBRD		
G. Billuris	S15	1
C. J. Brewer	S30	1
K. Chen	S30	1
E. E. Gerrels	S30	1
A. S. Gibson	S20	1
S. E. Hassett	S20	1
D. H. Holmes	S30	1
K. M. Horst	S06	1
A. Hunsbedt	S20	1
D. H. Imhoff	S64	1
Y. J. Lee	S30	1
D. E. Lutz	S20	1
P. M. Magee	S30	1
J. M. Roberts	S41	1
F. E. Tippets	S41	1
S. Wolf	S30	3
FBRD Library	S02	2